GOSPODARKA SUROWCAMI MINERALNYMI – MINERAL RESOURCES MANAGEMENT
2019 Volume 35 Issue 1 Pages 59–98
DOI: 10.24425/gsm.2019.128200

BEATA FIGARSKA-WARCHOŁ[1], GRAŻYNA STAŃCZAK[2]

The effect of petrographic characteristics on the physical and mechanical properties of currently exploited Pińczów Limestones – a type of Leitha Limestone (Carpathian Foredeep, southern Poland)

Introduction

Among the construction stone materials the Middle Miocene, organodetritic limestones enjoy unflagging popularity. This is due to their extremely high porosity and low bulk density, determining the favourable insulation properties, as well as susceptibility to processing, especially immediately after extraction. These limestone properties are the effect of the unique mineral-petrographic composition.

The Middle Miocene, shallow-water, detrital limestones, formed in the northern, marginal part of the Fore-Carpathian Basin, has been an important source of raw material in Poland for centuries. The subject of the economic interest in the Ponidzie area has been the red algal limestone facies known under the local name of Pińczów Limestone (sensu Studencki 1988a), a variety of the Leitha Limestone, which was described from the Vienna Basin (Kowalewski 1958; Krach 1962; Riegl and Piller 2000; Kováč et al. 2007; Wiedl et al. 2012). In the Wójcza-Pińczów Range, they form a horizontal strata, overlying the Mesozoic basement and building upper parts of hills with an angular unconformity (Fig. 1).

✉ Corresponding Author: Beata Figarska-Warchoł; e-mail: figarska@agh.edu.pl
[1] AGH University of Science and Technology, Kraków, Poland; ORCID: 0000-0002-6962-1775; e-mail: figarska@agh.edu.pl
[2] AGH University of Science and Technology, Kraków, Poland; ORCID: 0000-0002-6618-5998; e-mail: grazyna.stanczak.99@gmail.com

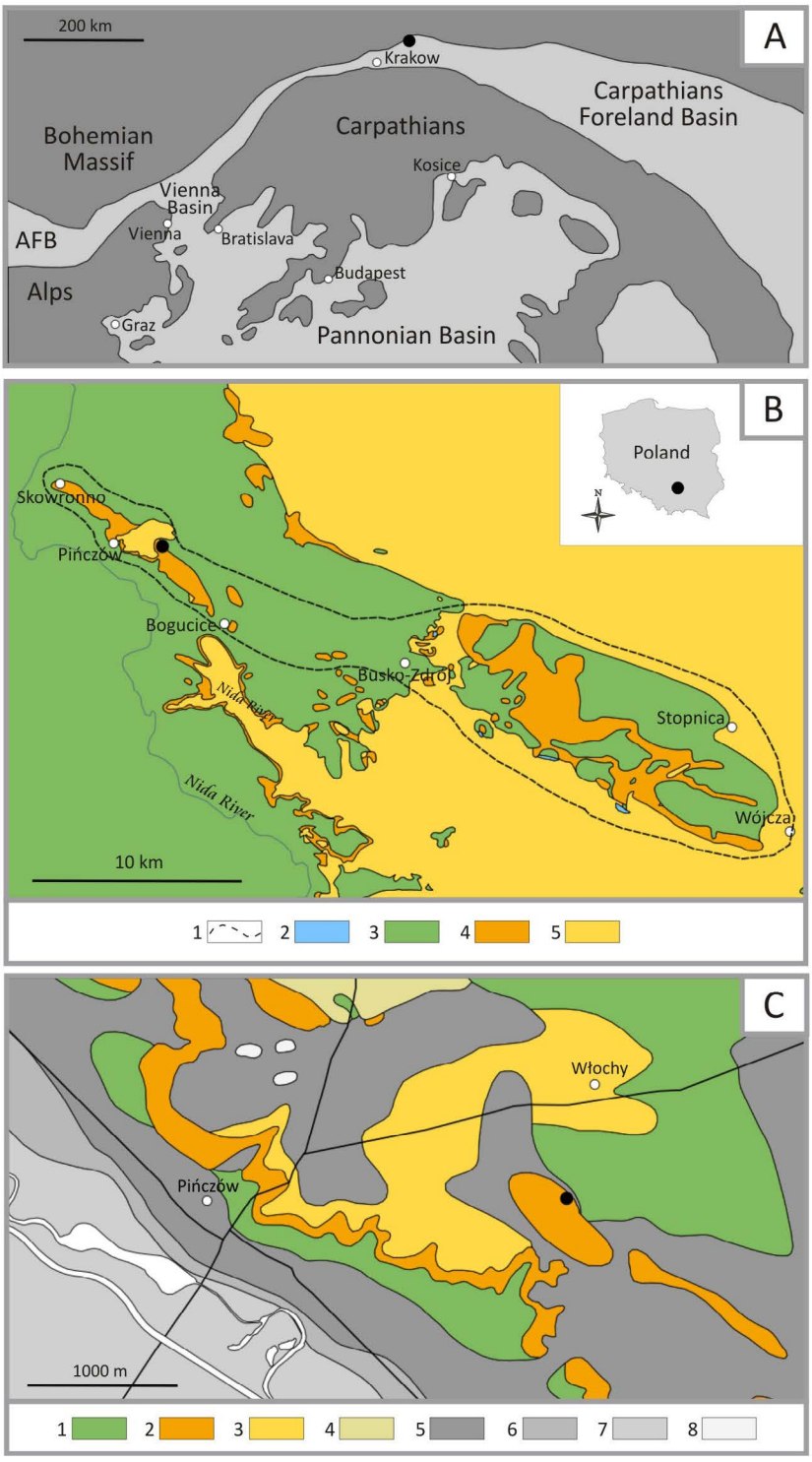
A
200 km
Krakow
Carpathians
Foreland Basin
Bohemian
Massif
Carpathians
Kosice
Vienna
Basin
AFB
Vienna
Bratislava
Budapest
Alps
Graz
Pannonian Basin
B
Poland
N
Skowronno
Pińczów
Bogucice
Busko-Zdrój
Nida River
Stopnica
Nida River
Wójcza
10 km
1
2
3
4
5
C
Włochy
Pińczów
1000 m
1
2
3
4
5
6
7
8

www.czasopisma.pan.pl PAN POLSKA AKADEMIA NAUK www.journals.pan.pl

Geological research in the area of Ponidzie has been carried out since the 19th century (vide Łyczewska 1975; Urban and Gągol 2015), and the Miocene rocks – their stratigraphy and geological structure, in particular within the Wójcza-Pińczów Range, were described in detail by Kowalewski (1958), Krach (1962), Radwański (1969), Areń (1971), Łyczewska (1971, 1972, 1975), Rydzewski (1975), Alexandrowicz et al. (1982), Drewniak (1994), Studencki (1979, 1988a, 1988b, 1999), Jasionowski (1997), Górka (2002) and Wysocka et al. (2016) and other authors.

The tradition of the exploitation and use of these rocks in both defensive and sacred buildings dates back to the beginnings of Polish statehood and was associated in the early Middle Ages with the castle in Wiślica. The period of greatest prosperity of the Pińczów stonemason's center took place in the 16th century due to the activity of Italian sculptors, using this limestone to make sophisticated stone elements for the decoration of castles, palaces as well as churches and monasteries. This is evidenced by numerous previously active quarries scattered between Skowronno near Pińczów and Kików near Stopnica (Penkalowa 1963; Weber-Kozińska 1963; Fijałkowska and Fijałkowski 1966; Gadomski 1970; Haber et al. 1991; Smoleńska and Rembiś 1999; Kardyś 2006; Rembiś and Smoleńska 2008; Rajchel 2014; Urban and Gągol 2015) (Fig. 1C). In recent decades, the exploitation of limestone has been limited to the: Skowronno, Pińczów, Bogucice and Włochy deposits, and only the latter is currently being operated (Bromowicz et al. 2004, 2005; Bromowicz and Figarska-Warchoł 2012; Szuflicki et al. eds. 2017). This material is presently highly desirable for conservation purposes, and also as building stone used in contemporary architecture.

Fig. 1. Location of the Middle Miocene red algal limestones cropping out in the studied Włochy quarry (black point).
A. Palaeogeography of the Carpathians Foreland Basin and Vienna Basin during the early Middle Miocene (Langhian Stage) after Jiménez-Moreno et al. (2006) and Rögl (1998); AFB – Alpine Foreland Basin.
B. The Wójcza-Pińczów Range (1), the Upper Jurassic carbonates (2), the Upper Cretaceous marls and marly chalks (3), the early Badenian Pińczów Formation (4), the other Neogene sediments (5), modified from Jurkiewicz and Woiński (1979).
C. Geological sketch map of the vicinity of Pińczów; the Upper Cretaceous marls, marly chalks, sandstones and gaizes (1), the early Badenian Pińczów Formation (2), the Sarmatian clay sediments (3), the Pleistocene loess (4), the Pleistocene glacial sands and gravels (5), the Pleistocene sands of accumulation terraces (6), the Holocene fluvial sediments (7), the Quaternary eolian sands, after Senkowicz (1958)

Rys. 1. Lokalizacja wapieni krasnorostowych środkowego miocenu wydobywanych w analizowanym kamieniołomie Włochy (czarny punkt).
A. Paleogeografia basenu przedkarpackiego i basenu wiedeńskiego we wczesnym miocenie środkowym (lang), AFB – basen przedalpejski;
B. Garb Wójczańsko-Pińczowski (1), górnojurajskie utwory węglanowe (2), górnokredowe margle i kreda marglista (3), dolnobadeńska formacja z Pińczowa (4), inne osady neogenu (5);
C. Szkic geologiczny okolicy Pińczowa; górnokredowe margle, kreda marglista, piaskowce i gezy (1), dolnobadeńska formacja z Pińczowa (2), osady ilaste sarmatu (3), plejstoceńskie lessy (4), plejstoceńskie piaski i żwiry lodowcowe (5), plejstoceńskie piaski teras akumulacyjnych (6), holoceńskie osady rzeczne (7) czwartorzędowe piaski eoliczne

The previous publications concerning the Pińczów Limestones focus on the microfacies and palaeogeographic analysis, while the petrographic variability issues in relation to physical and mechanical properties has not been the subject of research so far. However, these features are strictly connected with the durability of the stone material used in architecture both in the past and in the currently exploited limestones from the Włochy deposit. The aim of the research was to find a relationship between the petrography of the Miocene red algal Pińczów Limestones and their physical and mechanical properties. Additionally, on the basis of results published in literature, the quality of the raw rock material from the Włochy quarry has been compared to the other Leitha Limestones from the Polish part of the Carpathian Foredeep as well as from other European Badenian basins.

In the paper a detailed petrographic characteristics of distinguished limestone varieties have been presented. It included a granulometry analysis of skeletal components and a quantitative assessment of the mineral-petrographic composition of detritus and cements, as well as the contents of inter- and intragranular pores. The quantitative analysis basically carried out in the polarizing microscope, has been supplemented by the observations in the scanning electron microscope (SEM-EDS) to obtain the qualitative characteristics of the dominant clastic components that build the fabric of the limestones, as well as the clay and micrite matrix and sparite cement. The chemical analysis of the samples provided information on the main constituents of the samples and their solubility. The XRD method was used to identify mineral phases of solid samples and acid-insoluble matter.

Tests of density, water absorption and porosity of the samples enabled the relationship between the physical parameters and the petrographic characteristics of the investigated limestone varieties to be determined. On the basis of ultrasonic waves velocity and uniaxial compressive strength measurements, the variety of the most favourable mechanical properties has been indicated and the method of prediction of strength properties based on non-destructive tests has been proposed. A comparison of the obtained results with the properties of red algal limestones from the other deposits situated in the NW part of the Wójcza-Pińczów Range showed that the limestones from the Włochy deposit do not differ in quality from the previously used Pińczów Limestones (Penkalowa 1963; Dębski ed. 1966; Bugajska-Pająk 1974; Rutkowski 1980; Kozłowski 1986; Pinińska ed. 1994). They are also similar to the Leitha Limestones exploited in other European countries i.e. Austria, Czech Republic, Slovakia or Hungary (Török et al. 2004; Bednarik et al. 2014; Baud et al. 2017; Pápay and Török 2017).

1. Material and methods

1.1. Field observations and sampling

Field observations were carried out in 2017 in the Włochy limestone deposit, recognized in the years 2007–2011, in the place where the local exploitation was previously carried

out in an old quarry (Przybyszewski 2007; Przybyszewski and Wnęk-Potowniak 2011). The WGS84 coordinates of the quarry are: 50°31'19'' N, 20°33'28'' E (Fig. 1D).

In the mining excavation the detrital limestones of light beige colour with a yellowish shade and variable grain size have been outcropped. The totally thickness of the deposit ranges from 2.0 to 14.0 m. Layers of limestone have been underlaid by gray clays with rusty coatings, and their overburden with a thickness of 0.5–4.8 m consists of limestone debris and soil.

In the southern wall of the quarry, which was available for sampling, two beds of limestones with a thickness of 1.8 m and 2.0 m were exposed. The lower one (layer I) was characterized by a fine-detrital texture, while the upper (layer II) contained the coarser grains of the sizes up to a few mm. The small intensity of the vertical planes of discontinuity found in that part of quarry gives the possibility of obtaining blocks of relatively large dimensions (up to 3 m in length and over 1 m in height). The third, over a meter thick, layer of medium detrital limestones (layer III) with numerous horizontal discontinuities dividing the rock into small plates ended the deposit profile. In the western wall of the quarry, only a higher bed of blocky limestone (layer II) has been available to observations, much more intensely cut by joints in this place and overlaid by the layers of platy limestones (layer III) and debris.

The material for the study was taken from the lowest, thick bed (layer I), in the southern wall of the quarry (samples of series No. 200) and from the upper, thick bed from the western wall (layer II) (samples of series No. 300). Moreover, the subject of the tests have been samples originating from the marketable block of limestone previously extracted (probably from the lower thick layer I in the central part of the deposit) and processed in the masonry company (samples of series No. 100). All the samples were oriented towards the bedding (C) and to the main joint systems (A and B).

1.2. Petrographic studies

Two samples of variety No. 100 (samples No. 101 and 102) and individual samples of varieties No. 200 and 300 were selected for petrographic analysis. For each of them, thin sections impregnated with blue resin, and oriented perpendicularly (sections A and B) and parallel to the bedding (sections C), were prepared.

The microscopic investigations, including (1) the granulometry of the skeletal components and (2) the quantitative assessment of the mineral-petrographic composition of the detritus and cements, as well as the contents of the inter- and intragranular pores, were carried out in a polarizing microscope in a transmitted light on thin sections A or B. Detailed observations of the skeletal components, cements and pore space were made on thin sections and rock fragments using the FEI Quanta 200 FEG scanning elektron microscope.

The granulometric measurements were made for three hundred consecutive detrital components of sizes of at least 31 μm, cut by a scanline situated perpendicular to the bedding. Each clastic component was identified and measured in terms of its maximum diameter or

internal axis length in the case they were deformed. The dimensions of detrital components measured in this way and converted to phi (φ) units, were used to calculate the statistical grain size measures according to the original Folk and Ward (1957) formulas such as graphical mean grain size (GM, φ), graphical standard deviation (GSD, φ) and graphical skewness (GSk). Microscopic granulometric measurements were made using a Nikon DS-Fi1 digital camera coupled with a polarizing microscope and the NIS-Elements BR image analysis software tools (Stańczak and Figarska-Warchoł 2016).

The quantitative analysis was performed on the same thin sections for which the granulometric measurements were performed. The point counting method was applied in a regular grid of 0.4 × 0.6 mm and 0.6 × 0.6 mm, respectively for finer and coarser grained rocks, identifying a clastic component, cement, matrix or pores at each grid node. The fragments of the bioclast shells found in the nodes were classified to the appropriate group of skeletal components, while the inside parts of the bioclasts, empty or filled with a mineral substance, were classified as intragranular pores or as cement or matrix (grain-solid measurements). In each thin section, the analysis was carried out until the amount of 500 points were identified as a mineral component (bioclast, detrital grain or cement), and the pores counted during the analysis increased the sum of counts above this value (550–581), respectively, were obtained. Therefore, the grid covered a fragment of a thin section of an area of 120 to 190 mm^2. The percentage of a given component in the rock (p) and its accuracy ($p \pm 2\sigma$) were calculated on the basis of the obtained counts (Van der Plas and Tobi 1965). The percentage mineral composition of limestones was calculated for the sum of all mineral components (MPh = bioclasts + detrital grains + matrix + cements) equal to 100%, whereas the percentage of pores were assessed for the sum of mineral components and pores (MPh + P) equal to 100%.

Skeletal components of organic and terrigeneous origin were taken into account in the granulometric analysis and in the quantitative assessment of mineral composition. Based on the diagnostic features described in the available literature, organic skeleton remains were identified (Milliman 1974; Bathurst 1975; Adams et al. 1991; Flügel 2004; Adams and MacKenzie 2011). Moreover, the class of unidentified bioclasts was distinguished. Their small sizes as well as the lack of characteristic features did not allow them to be assigned to any of the recognized groups of organisms. In the quantitative analysis microsparite intergranular and intragranular cement (inside organic debris) was distinguished, as well as syntaxial sparite cement developed in the form of overgrowths on the remains of echinoids and matrix.

1.3. Chemical and phase composition

The purpose of the chemical tests of limestones was to determine the amount of insoluble matter that does not dissolve in 10% hydrochloric acid solution. In order to do that, the powdered samples of limestones were dissolved in 10% HCl for 24 h and then the dried residues

were weighed. Moreover, the content of carbonaceous material and loss on ignition (LOI) were also determined. The first one required heating powdered samples in air atmosphere at 375º ± 5º for 16 h (Keeling 1962), and the second – ignition at 1000º ± 5º for 2 h. It allowed the amount of calcium carbonate to be estimated.

The filtered (0.45 µm) water solutions obtained by dissolution of 20 ± 0.01 g of dried to constant weight limestone aggregate (fraction of 2–5 mm) in 50 ml of distilled water, lasting for 72 h at normal atmospheric pressure and temperature approx. 21ºC, were subjected to chemical tests using optical atomic emission spectroscopy with the ICP-OES Optima 7300 DV PerkinElmer's device.

The identification of mineral phases in solid samples and acid-insoluble matter was supported by the X-ray diffraction conducted on the basis of the Debye-Sherrer powder method, using the DRON 3.0 device with Cu Kα radiation recorded for untreated and glycolated samples in the range of 2–75º 2θ and 2–20º 2θ, respectively.

1.4. Apparent density and water absorption

Apparent density and water absorption at atmospheric pressure tests were carried out according to the Polish technical standards (PN-EN 1936; PN-EN 13755) on the cubic specimens with the side length of 70 ± 5 mm.

1.5. Open and total porosity

The open porosity available for water and the total porosity (PN-EN 1936) were measured, accepting the value of the specific density of limestone equal to 2.70 Mg/m^3 for calculations (according to Przybyszewski 2007).

Using an automatic PoreMaster 60 mercury intrusion porosimeter (Quantachrome Instruments) the pore size distribution was obtained and the total porosity was calculated taking the total pore volume into account. The porosimeter tests were carried out in the pressure range of 0.06–204 MPa (the pore diameter range from approximately 200 mm to 6 nm) and the values for the surface tension of mercury of 480 mN/m and a contact angle on rock of 130° were used in calculations.

1.6. Capillary water absorption

The water absorption coefficient by capillarity [g/m^{2}s$^{0.5}$] calculated as the weight increase of water absorbed by a rock sample in the function of the area of its immersed base and the time (PN-EN 1925) was determined for selected cubic samples on the 70 ± 5 mm side, cut from material used by the masonry company and from the material collected in the

quarry. For the samples of all varieties, the immersed base was the surface parallel to the bedding, while for the samples of the variety No. 100, the base was additionally perpendicular to the bedding.

The rate of the capillary rise of water [cm/min] up to a sample height of 30 cm was investigated. For this purpose, dried samples in the form of beams of 50 × 50 × 300 (± 5) mm were immersed in water to a depth of 3 ± 1 mm, constantly maintaining that level. At increasing time intervals, the height (with accuracy up to 0.1 cm) from the water table to the highest point of the zone saturated with capillary water, visible on the side wall of the sample, was measured.

1.7. Velocity of longitudinal ultrasonic waves

For the oriented, cubic samples of 70 ± 5 mm side length, the velocity of longitudinal ultrasonic waves (V_L) was determined (PN-EN 14579). The Unipan-Ultrasonic devices with a pair of 500 MHz transducers (with 20 mm diameter) was used to measure the time of the ultrasonic wave transition. The direct ultrasonic tests were performed, in three mutually perpendicular directions, for the air-dried samples of all varieties and for the water-saturated samples exclusively of variety No. 100.

1.8. Uniaxial compressive strength

The uniaxial compressive strength (UCS) has been determined only for the cubic samples (70 ± 5 mm) taken from the masonry company (variety No. 100) in the dry and water-saturated state (PN-EN 1926). The direction of the applied load was parallel or perpendicular to the bedding.

2. Results and discussion

2.1. Lithology

In the dry state, the tested limestone samples were light beige, although varieties No. 100 and 200 were characterized by a yellowish shade (more intense for 200), and variety No. 300 was distinguished by its brightest, almost white, colour. After soaking samples in water, the colour of varieties No. 100 and 200 became more yellowish, while the colour of variety No. 300 did not change. The horizontal or oblique laminae with a thickness of 1 mm were observed in all samples, especially in wet ones, and manifested by a slight change in colour towards yellowish shades.

In many samples, there were rectilinear, thin (approx. 1 mm), mineralized zones oriented in various directions, whose boundaries were poorly discernible. Furthermore, in the samples of varieties No. 200 and 300, there were very fine, dark, almost black, grains dispersed in rock, and in variety No. 200 they were slightly more numerous. The detrital components of the samples of limestone varieties No. 100 and 200 were relatively the best sorted and fine-grained; therefore, it was difficult to recognize the organic remains in the macroscopic observation and to notice the directional arrangement of the sporadically occurring larger grains. On the other hand, samples of variety No. 300 were distinguished by the most coarse grained clastic material and its poor sorting, with the macroscopically visible randomly distributed, crumbled organic remains.

2.2. Petrographic analysis

2.2.1. Grain size

On the basis of granulometric analysis (Table 1) it was found that limestone of variety No. 300 was characterized by the most coarse grained (GM = 0.943 φ – the most coarse fractions of coarse sand) and poorly sorted of the clastic material (GSD = 1.348 φ), as well as the largest negative skewness to coarser fractions (GSk = –0.284) (Table 2). Such a granulometric characteristic of variety No. 300 was the result of the presence of numerous components such as red algae, foraminifera and the largest of them: bryozoans and echinoids, whose sizes reached approx. 6 mm, with an average size of 1.56 mm and 0.75 mm, respectively (Table 1).

On the contrary, the clastic material of the variety No. 200 was characterized by the finest grain size (GM = 2.503 φ – finer fractions of fine sand) and moderate sorting (GSD = 0.954 φ), with almost symmetrical grain size distribution (GSk = –0.092) (Table 2). Almost half of the measured components were foraminifera, the size of which reached up to 1.80 mm, and their average diameter (0.23 mm) was the lowest among the samples measured. Quartz grains, with the average size of 0.11 mm, belonged to the smallest components. The sizes of the other components did not exceed 1 mm, and their average size ranged from 0.27 mm to 0.47 mm (Table 1).

The third of the analysed limestone varieties (represented by samples No. 101 and 102) revealed the intermediate grain size parameters, because it had had the poorly sorted clastic material (GSD equal to 1.196 φ) with the mean grain diameter belonging to coarser fractions of fine sand (GM equal to 2.250 φ). The negative value of the GSk parameter (–0.233) indicated that the particle size distributions of these samples were skewed towards coarser fractions. The size of numerous foraminifera, the remains of which were much larger than in sample No. 200, had a slight effect on the grain size of limestone variety No. 100. However, the presence of large remains of red algae, bivalves and sporadic foraminifera resulted in the poor sorting and negative skewness of these limestones.

Table 1. Granulometric analysis of major components of the limestones from the Włochy deposit

Tabela 1. Analiza granulometryczna głównych składników wapieni ze złoża Włochy

Components	Fora-minifera	Red Algae	Echinoids	Bivalves	Quartz	Bryozoans	Cirriedians
Variety No. 100							
Count	119	33	47	33	39	4	4
Average size [mm]	0.48	0.50	0.31	0.38	0.10	0.37	0.30
Min – Max [mm]	0.06–5.79	0.10–1.22	0.05–5.29	0.06–1.10	0.03–0.22	0.28–0.47	0.22–0.37
Variety No. 200							
Count	144	20	39	18	47	6	5
Average size [mm]	0.23	0.35	0.27	0.36	0.11	0.27	0.47
Min – Max [mm]	0.05–1.80	0.11–0.84	0.04–0.87	0.15–1.02	0.05–0.18	0.19–0.44	0.31–0.71
Variety No. 300							
Count	85	102	25	17	1	31	30
Average size [mm]	0.74	0.86	0.75	0.86	0.12	1.56	0.63
Min – Max [mm]	0.13–3.90	0.09–3.04	0.16–6.88	0.20–2.09	0.12	0.19–5.76	0.20–5.09

Table 2. Statistical grain size measures (according to the original Folk and Ward 1957 formulas) of limestones from the Włochy deposit

Tabela 2. Graficzne parametry uziarnienia wapieni ze złoża Włochy

Variety No.	100	200	300
Number of particles	300	300	300
GM (Φ)	2.250	2.503	0.943
GM within class of:	fine-grained sand 2–3 φ		coarse-grained sand 0–1 φ
GSD (Φ)	1.196	0.954	1.348
Sorting	poor	moderate	poor
GSk	**– 0.233**	**– 0.092**	**– 0.284**
Skewness	coarse skewed	near symmetrical	coarse skewed

GM – graphical mean grain size, GSD – graphical standard deviation, GSk – graphical skewness.

For the examined limestone samples, the correlation between the GM, GSD and GSk was found, as it was previously noticed and described for siliciclastic rocks by the Bromowicz (1974), Peszat (1984), Stańczak (2008), Stańczak and Figarska-Warchoł (2016) and Figarska-Warchoł and Stańczak (2016). The obtained results showed that with the decrease in the mean size of grains (GM increase, φ) the sorting is improved (GSD decrease, φ) and the GSk parameter value increases, which means the transition from the negatively skewed grain size distributions for coarse-grained samples to symmetric distributions for the finer-grained.

2.2.2. Variability of mineral composition

In the quantitative analysis of the solid mineral phase (MPh = 100%) a sample of variety No. 300 was distinguished by a significant domination of the sum of red algae, bryozoans and foraminifera (64.4%) over the sum of other bioclasts (10.6%) with a small proportion of inorganic grains (1.4%) (Table 3). In the samples of varieties No. 100 and 200, the first of them reached the level of 31.6–33.9%, while the percentage of other bioclasts fluctuated within the range of 21.8–23.6%, with a relatively similar content of quartz and other detrital grains (7.6–7.7%).

The variability of the content of the three dominant organodetrital components, such as red algae, bryozoans and foraminifera, allowed samples of varieties No. 100 and 200, which consisted in majority of foraminifera (21.5–22.8%) and red algae (8.0–12.2%), with a negligible content of bryozoans (less than 1%) to be distinguished, while in sample 300, red algae (35.0%) predominated over foraminifera (16.0%) and bryozoans (13.4%). Among the foraminifera, the percentage of small tests was the highest in the finest-grained sample of variety No. 200 (11.2%) and it significantly prevailed over the percentage of large benthic foraminifera (3.0%), whereas in the coarse-grained sample No. 300, benthic foraminifera were dominant (7.6%).

The contents of organodetrital components, matrix and cements in samples of varieties No. 100 and 200 were similar, whereas in sample No. 300 the predominance of skeletal components (75.0%) over the matrix (8.4%) and the sum of cements (15.2%) was found. A quantitative analysis of the cement content for all the samples indicated the predominance of microsparite developed in the intergranular space (11.6–18.0%) over the intragranular (2.6–5.3%) and overgowth cement developed on the remains of echinoids (1.0–3.9%). The analysis of the variability of the sum of matrix and cements in the function of the GM parameter showed that the amount of binders increases ($R^2 = 0.97$) with the decrease in grain size (GM increase, φ). Similar relationships were found for sandstones (Figarska-Warchoł and Stańczak 2016).

As a result of quantitative analysis including a solid mineral phase and pores (MPh + + P = 100%), it was found that the finest-grained sample No. 200 had the highest content of pores (13.9%), among which the intergranular (11.7%) prevailed over the intragranular ones (2.2%), mainly inside the small and large foraminifera (Table 3). In the fine-grained samples of variety No. 100 with poor sorting of the clastic material, the total pore content was slightly

lower and amounted to 11.1%, of which the intergranular pores constitute 8.0%, while the intragranular 3.1%. The intragranular pores in samples of varieties No. 100 and 200 were recorded inside the foraminifera tests (1.9–2.8%), and subordinately as cavities in serpulid tubes, in barnacle tests and in the structure of red algae and bryozoans (in total 0.4%). On the other hand, the coarse-grained sample No. 300, in which the sorting of the grains was poor, had the lowest content of pores (9.1%), with the comparable share of intergranular (4.7%) and intragranular (4.4%) ones. The latter were registered mainly in the bryozoans (2.5%), large (1.3%) and small (0.4%) foraminifera, as well as red algae (0.2%). The presented information confirms the relationships found between the mean grain diameter (GM, φ), graphical standard deviation (GSD, φ) and the content of intergranular pores (P-inter, %) determined on the basis of the thin sections analysis (Fig. 2).

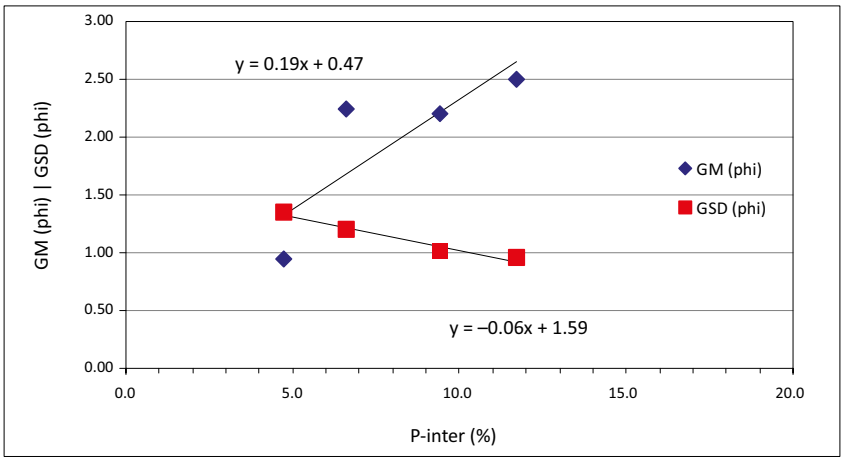

Fig. 2. Relationship between graphical mean grain size (GM, φ), graphical standard deviation (GSD, φ) and the content of intergranular pores (P-inter, %) quantitatively determined in thin sections

Rys. 2. Zależność pomiędzy średnią graficzną średnicą ziaren (GM, φ) oraz graficznym odchyleniem standardowym (GSD, φ) a udziałem porów międzyziarnowych (P-inter, %) oznaczonych ilościowo w płytkach cienkich

On the basis of the results of the granulometric analysis (Table 1, 2) and the contents of clastic components building the rock fabric (Table 3), it can be concluded that the limestone samples belonging to the three analyzed varieties (100, 200 and 300) represent organodetrital facies of different grain size and sorting, starting from the fraction of coarse sand of poor sorting (variety No. 300), through a poorly sorted fine sand (variety No. 100), and ending with a moderately sorted fine sand (variety No. 200). Similar fractions within the organodetrital facies of the Leitha Limestones were distinguished in research previously conducted by other authors (Dullo 1983; Studencki 1988a 1999; Drewniak 1994; Doláková et al. 2008; Wiedl et al. 2012).

Table 3. Mineral phase (MPh) composition and pore content (P) of the limestones from the Włochy deposit

Tabela 3. Skład fazy mineralnej (MPh) i udziału porów (P) wapienie ze złoża Włochy

Variety No.		100	200	300
		p (%) ± 2σ	p (%) ± 2σ	p (%) ± 2σ
		MPh = 100%		
Bioclasts	Red algae	**12.2** ± 2.88	**8.0** ± 2.43	**35.0** ± 4.27
	Bryozoans	**0.2** ± 0.40	**0.8** ± 0.80	**13.4** ± 3.05
	Foraminifera (sum):	**21.5** ± 3.67	**22.8** ± 3.75	**16.0** ± 3.28
	◆ small tests	7.2	11.2	2.8
	◆ large tests	8.7	3.0	7.6
	◆ fragments	5.6	8.6	5.6
	Echinoids	**9.2** ± 2.58	**15.2** ± 3.21	**4.2** ± 1.79
	Bivalves	**3.7** ± 1.68	**1.6** ± 1.12	**2.2** ± 1.31
	Cirripedians	**4.7** ± 1.71	**1.2** ± 0.97	**1.4** ± 1.05
	Other bioclasts (sum):	**1.5** ± 1.06	**2.0** ± 1.25	**2.2** ± 1.31
	◆ serpulids	0.4	0.0	0.6
	◆ sponge spicules	0.1	0.0	0.0
	◆ brachiopods	0.0	0.0	0.2
	◆ corals	1.0	2.0	1.4
	Unidentified bioclasts	**2.7** ± 1.44	**3.6** ± 1.67	**0.6** ± 0.69
Detrital grains	Quartz	**5.3** ± 1.99	**6.0** ± 2.12	**0.0** ± 0.00
	Other detrital grains (sum):	**2.4** ± 1.37	**1.6** ± 1.12	**1.4** ± 1.05
	◆ feldspars	0.0	0.4	0.2
	◆ glauconite	0.8	0.8	0.8
	◆ pirite	0.5	0.0	0.4
	◆ abraded calcitic monocystals	0.8	0.4	0.0
	◆ aggregates	0.1	0.0	0.0
	◆ heavy minerals	0.2	0.0	0.0
Matrix and Cements	Matrix	14.7 ± 3.17	12.6 ± 2.97	8.4 ± 2.48
	Sparite inter- and intragranular cements (sum)	21.9 ± 3.70	24.6 ± 3.85	15.2 ± 3.21
	Microsparite intergranular cement	12.7 ± 2.97	18.0 ± 3.44	11.6 ± 2.86
	Syntaxial sparite overgrowths on echinoids	3.9 ± 1.73	2.6 ± 1.42	1.0 ± 0.89

Table 3. cont.

Tabela 3. cd.

Variety No.		100	200	300
		p (%) ± 2σ	p (%) ± 2σ	p (%) ± 2σ
		MPh = 100%		
Matrix and Cements	Microsparite intragranular cement – inside:	**5.3** ± 2.01	**4.0** ± 1.75	**2.6** ± 1.42
	◆ bryozoans	0.1	0.2	1.2
	◆ tests of small foraminifera	4.0	3.4	0.4
	◆ tests of large foraminifera	1.0	0.2	0.6
	◆ shells of cirripedians	0.2	0.2	0.4
		MPh + P = 100%		
	MPh =	**88.9** ± 2.65	**86.1** ± 2.87	**90.9** ± 2.45
Pores	Inter- and intragranular pores (sum)	11.1 ± 2.65	13.9 ± 2.87	9.1 ± 2.45
	Intergranular pores	8.0 ± 2.28	11.7 ± 2.67	**4.7** ± 1.81
	◆ interparticle pores	7.9	11.2	4.5
	◆ moldic pores	0.1	0.5	0.0
	◆ shelter pores	0.0	0.0	0.2
	Intragranular pores – within:	3.1 ± 1.43	2.2 ± 1.23	**4.4** ± 1.74
	◆ red algae	0.2	0.0	0.2
	◆ bryozoans	0.0	0.2	2.5
	◆ tests of small foraminifera	1.0	1.0	0.4
	◆ tests of large foraminifera	1.8	0.9	1.3
	◆ tubes of serpulids	0.1	0.0	0.0
	◆ shells of cirripedians	0.1	0.2	0.0

MPh = Bioclasts + Detrital Grains + Matrix + Cements;
P = Pores;
p – the percentage of a component in the rock and its accuracy (p ± 2σ) calculated according to van der Plas and Tobi (1965).

In the Dunham classification (1962), modified by Embry and Klovan (1971), the sample of variety No. 300 represents poorly sorted bioclastic calcarenite of rudstone type and a red algal-foraminiferal-bryozoic composition with the domination of the large benthic foraminifera over fine foraminifera and a small admixture of the remains of echinoids (Table 3).

On the other hand, samples of varieties No. 100 and 200 represent the poorly and moderately sorted calcarenites of packstone type which have a foraminiferal-red algal-echinoidal composition with almost equal content of large and fine foraminifera (variety No. 100), or the skeletal grain association is distinguished by a foraminiferal-echinoidal-red algal composition with the abundance of small foraminifera over large ones (variety No. 200). The biodetritus identified in thin sections corresponded to the flora and fauna associations described in the Miocene limestone of the Wójcza-Pińczów Range (Rydzewski 1975; Drewniak 1994; Studencki 1988a, b, 1999).

2.2.3. Characteristics of the selected granular components

Red algae observed in the sample of variety No. 300 were represented mainly by elongated branching forms and rounded nodular rhodoids reaching the size up to a few millimeters, and subordinately by their more fragmented remains, which dominate in samples of varieties No. 100 and 200. All forms of red algae showed a different preservation state of reticular structure of their carbonate skeletons. The most compact and rigid fragments were observed in sample No. 300, where the internal parts of the cells and, to a lesser extent, their walls were almost completely filled with carbonate crystals (Fig. 3A, 3B). On the other hand, in the finest grained sample No. 200, the reticular structure of these algae was strongly disintegrated and therefore difficult to recognize (Fig. 3C, 3D). However, in the fine-grained samples of variety No. 100, the structure of these algae was partially porous.

Foraminifera were represented by a large association of very different test shapes, whose observed forms and arrangement of the chambers depended on the orientation of the remains in relation to the thin section plane (Fig. 3E, 3F). The largest of them are benthic foraminifera, whose tests with relatively thick walls, had discoidal or lenticular shapes with a planspiral arrangement of chambers, or conical (trochospiral) or cylindrical with uniserial or biserial chambers. The small foraminifera were characterized by thin tests and were usually isometric. Perforations as well as inclusions were observed within the walls of large and small foraminifera.

Bryozoans were merely significant in sample No. 300, where nodular or elongated carbonate skeletons with fan-like or radial tube arrangement or, less frequently, bifoliated forms were found (Fig. 4C). Zooecia had round or oval shapes with dimensions up to 0.6 mm.

Quartz grains, representing one of the finest detrital components, were dispersed among bioclasts or formed more or less abundant accumulations (Fig. 3E, 3F). Most of the grains were angular, and only some were well rounded; they were also often fractured.

2.2.4. The qualitative characteristics of the limestone fabric and cement

The fabric of the coarse-grained limestones of variety No. 300 were built with randomly distributed fragments of red algae as well as accompanying them bryozoic remains and the specimens of large benthic foraminifera, which were complimented by their fine-grained

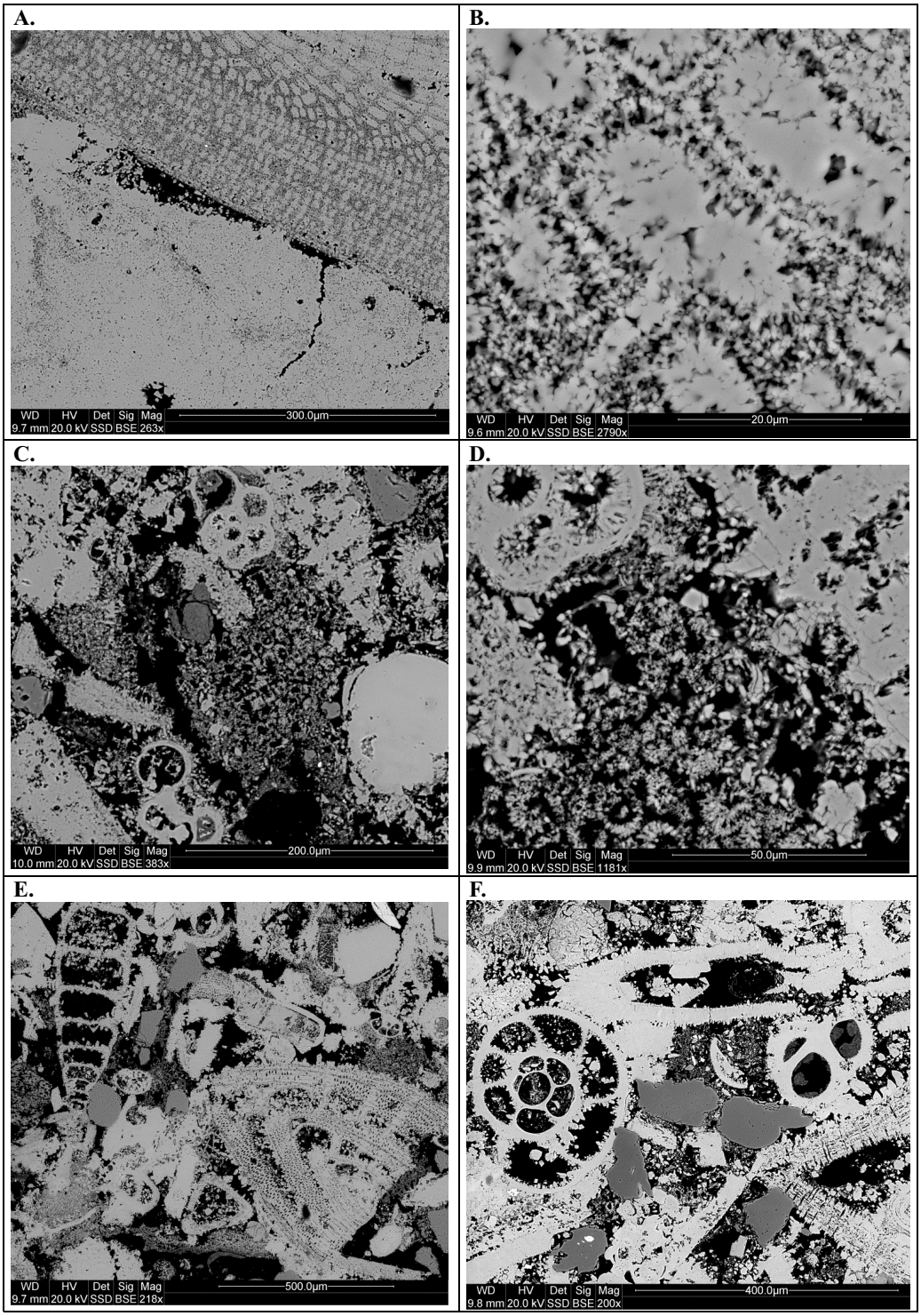
A.
WD HV Det Sig Mag
9.7 mm 20.0 kV SSD BSE 263x
300.0µm
B.
WD HV Det Sig Mag
9.6 mm 20.0 kV SSD BSE 2790x
20.0µm
C.
WD HV Det Sig Mag
10.0 mm 20.0 kV SSD BSE 383x
200.0µm
D.
WD HV Det Sig Mag
9.9 mm 20.0 kV SSD BSE 1181x
50.0µm
E.
WD HV Det Sig Mag
9.7 mm 20.0 kV SSD BSE 218x
500.0µm
F.
WD HV Det Sig Mag
9.8 mm 20.0 kV SSD BSE 200x
400.0µm

counterparts and fragments of echinoids, bivalves, barnacles, and tests of small foraminifera (Fig. 4C). In turn, the skeleton of fine-grained limestones of poor sorting of variety No. 100 was built mainly with foraminifera which predominated over the detritus of red algae, echinoids, bivalves and quartz grains (Fig. 4A). Larger, flat and elongated remains (mainly discoidal foraminifera) were usually arranged parallel and rarely oblique to the bedding. In fine-grained limestone with moderate sorting (variety No. 200), small foraminifera and fragments of larger foraminifera, as well as quartz grains and remains of echinoids and red algae were the main components of the skeleton (Fig. 4B). Occasionally observed larger grains were arranged linearly, parallel to the bedding (Fig. 4A).

Detailed investigations of the binders in the scanning microscope enabled identification of the micrite and clay matrix. The first, in samples of variety No. 300, represented aggregates of crypto- and microcrystalline forms of calcium carbonate, which in the intergranular space formed the groundmass. The clay matrix was formed by aggregates of very fine flakes of clay minerals, among which very fine detrital grains were found. That material of variable composition was mainly accumulated inside the bryozoans zooecia and microborings, filling them almost completely or only partially, and it was found marginally in the intergranular space (Fig. 4C). The glauconization process of the clay matrix inside the bryozoan zooecia was observed, with some of these voids occupied by fully developed glauconite grains. The presence of iron compounds was marked both in the clay matrix and in the glauconite (Fig. 4E, 4F).

The cement in sample No. 300 occurred predominantly as intergranular microsparite. It precipitated on carbonate detrital grains as the acute and elongated crystals (size 5–30 μm) growing normal or subnormal to the surface of the bioclast (cement of dog tooth type).

Fig. 3. Diversity of the internal structure of the red algae thalli and the foraminifera tests from the organodetrital limestones observed in thin sections under scanning electron microscope. Photos by G. Stańczak (A–E) and A. Gaweł (F).
A – ridged and compact structure of the red algal thalli in contact to the bryozan fragment (sample 300). B – cellular structure of the red algal thalii is almost entirely filled by scalenohedral calcite (close-up of Fig. 3A). C – fragment of a red algal thalli strongly disintegrated and highly porous (sample 200). D – the internal structure of the red algal thalii (magnified part of Fig. 3C). Various shapes of foraminifera tests and quartz grains (dark grey): E – thin section parallel to the bedding plane (sample 101); F – thin section perpendicular to the bedding plane (sample 102)

Rys. 3. Zróżnicowanie wewnętrznej struktury krasnorostów i otwornic w wapieniach organodetrytycznych obserwowane w płytkach cienkich w mikroskopie skaningowym. Fot. G. Stańczak (A–E) i A. Gaweł (F).
A – zbita i sztywna struktura plechy krasnorostu w kontakcie z fragmentem mszywiołu (próba 300). B – komórkowa struktura plechy krasnorostu niemal całkowicie wypełniona kalcytowymi skalenoedrami (powiększenie rys. 3A). C – fragment silnie zdezintegrowanej i porowatej plechy krasnorostu (próba 200). D – wewnętrzna struktura plechy krasnorostu (powiększenie Rys. 3C). Zróżnicowane kształty otwornic i ziaren kwarcu (ciemnoszary): E – płytka cienka równoległa do płaszczyzny uławicenia (próba 101), F – płytka cienka prostopadła do płaszczyzny uławicenia (próba 102)

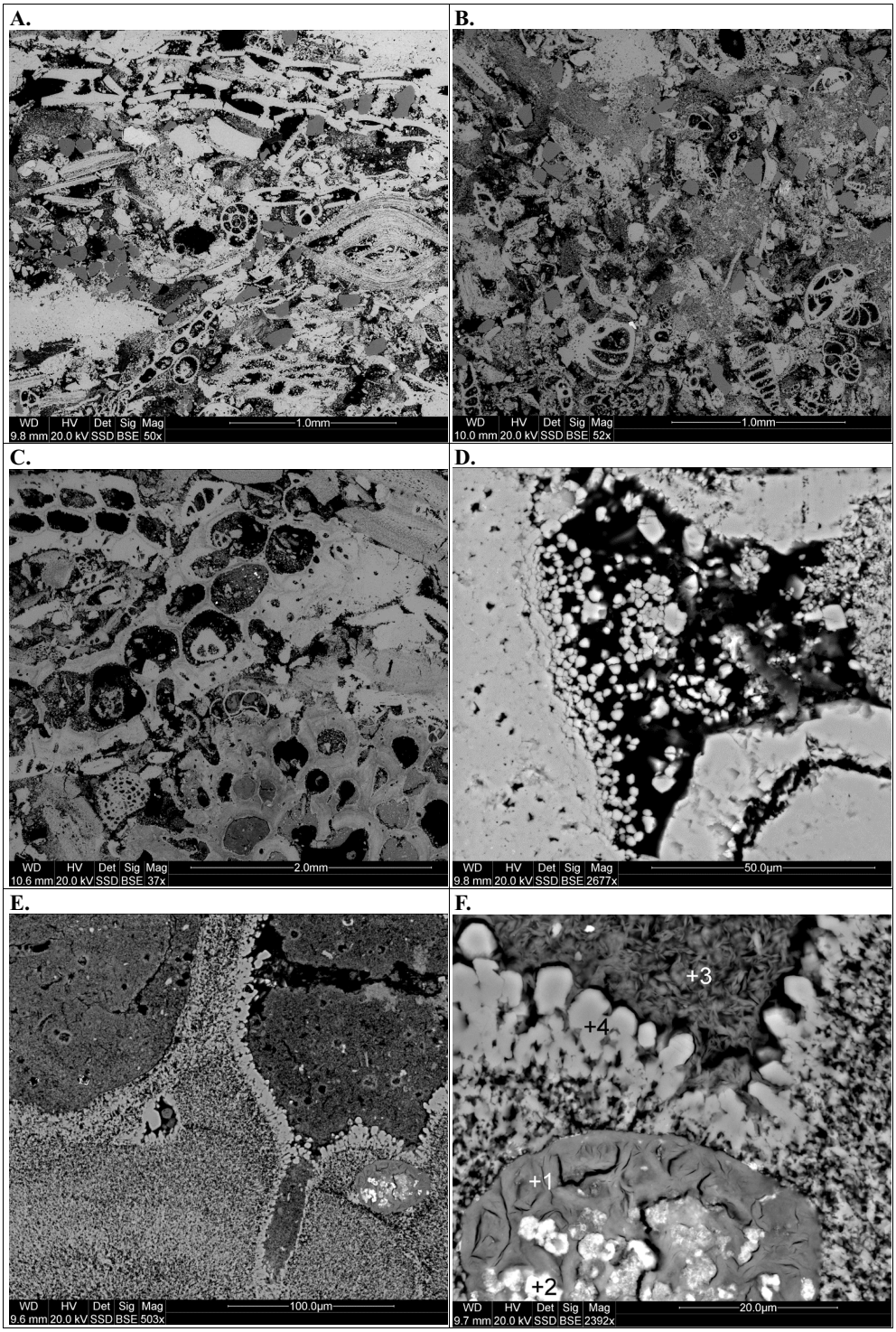
A.
WD HV Det Sig Mag
9.8 mm 20.0 kV SSD BSE 50x
1.0mm
B.
WD HV Det Sig Mag
10.0 mm 20.0 kV SSD BSE 52x
1.0mm
C.
WD HV Det Sig Mag
10.6 mm 20.0 kV SSD BSE 37x
2.0mm
D.
WD HV Det Sig Mag
9.8 mm 20.0 kV SSD BSE 2677x
50.0µm
E.
WD HV Det Sig Mag
9.6 mm 20.0 kV SSD BSE 503x
100.0µm
F.
+3
+4
+1
+2
WD HV Det Sig Mag
9.7 mm 20.0 kV SSD BSE 2392x
20.0µm

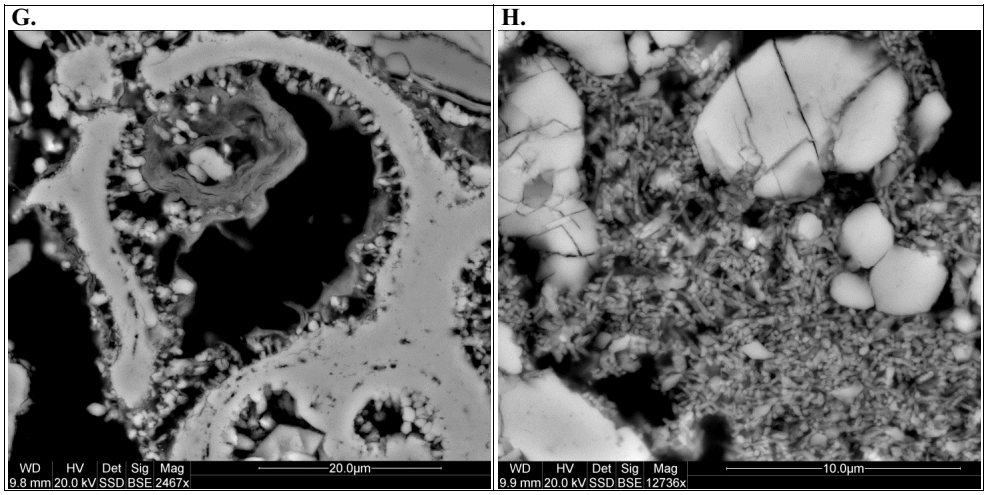

Fig. 4. Diversity of the fabric of organodetrital limestones (A–C) and their cements (D–H) observed in thin sections under scanning electron microscope. Photos by G. Stańczak (B–H) and A. Gaweł (A).
Rock fabric of the three varieties of limestone studied in thin section cut perpendicular to the bedding plane: A – fine-grained limestone with poor sorting and linearly arranged larger fragments of foraminifera (sample 102); B – moderately sorted fine-grained limestone with high amount of matrix and cements (sample 200), C – coarse-grained limestone with poorly sorted and chaotic arranged nodular or elongated skeletal fragments of bryozoans (sample 300). D – mikrospar dispersed in pore space bordering a foraminiferal test and syntaxial rim cement around an echinoid fragment (sample 101). E – zooecium filled with clay matrix, and its wall covered by microspar (sample 300). F – detail of the texture of clay matrix (3); bladed microspar (4) linning the wall of the bryozoan zooecium; glauconite (1) with iron compounds (2) filling a microboring within bryozoan skeleton (close-up of the lower right corner of Fig. 4E). G – the chamber of foraminiferal test is lining by the microspar perpendicular to the inside wall of the chamber; the rim of clays covers the microspars inhibiting their growth (sample 200). H – the internal texture of micritic matrix and microspar (intergranular groundmass) (sample 101)

Rys. 4. Zróżnicowanie więźby wapieni organodetrytycznych (A–C) i ich spoiw (D–H) obserwowane w mikroskopie skaningowym w płytkach cienkich prostopadłych do płaszczyzny uławicenia. Fot. A. Gaweł (A) i G. Stańczak (B–H).
A – słabo wysortowany wapień drobnoziarnisty z liniowo ułożonymi większymi fragmentami otwornic (próba 102). B – średnio wysortowany wapień drobnoziarnisty z dużym udziałem matriks i cementu sparytowego (próba 200). C – słabo wysortowany gruboziarnisty wapień z chaotycznie ułożonymi gruzłowatymi lub wydłużonymi fragmentami mszywiołów (próba 300). D – mikrosparyt rozproszony w przestrzeni porowej graniczący z okazem otwornicy i obwódka cementu syntaksjalnego wokół fragmentu jeżowca (próba 101). E – wnętrze zooecjum wypełnione przez ilastą matriks oraz jego ściany pokryte przez mikrosparyt (próba 300). F – szczegóły teksturalne ilastej matriks (3); listkowy mikrosparyt (4) wyścielający ścianę zoecjum mszywioła; glaukonit (1) ze związkami żelaza (2), wypełniający mikrodrążenia w obrębie szkieletu mszywiołu (powiększenie prawego dolnego narożnika Rys. 4E). G – komora otwornicy wyścielana przez mikrosparyt, narastający prostopadle do jej wewnętrznej ściany; obwódka ilasta pokrywająca mikrosparyt hamuje jego wzrost (próba 200). H – wewnętrzna tekstura mikrytowej matriks i mikrosparytu (spoiwo międzyziarnowe) (próba 101)

In all samples the microsparite cement also formed the isometric crystals with a diameter of several micrometres, which developed on the surface of carbonate bioclasts or were dispersed in the intergranular space or formed aggregates in it, connecting with larger sparite crystals (Fig. 4D). This microsparite also impregnated the micrite.

SEM observations revealed that the intragranular microsparite in sample No. 300 usually lined the inner walls of the bryozoan zooecia (Fig. 4E, 4F). These crystals had the shape of a blade or sword and formed isopachous fringe expanded towards the inside of voids. In contrast, the intragranular microsparite cement in the samples of varieties No. 100 and 200 precipitated in the chambers of foraminifera in the form of much finer crystals with a columnar or isometric shape, which gradually filled the space of the chamber until its complete occupation. Larger microsparite crystals appeared in the chambers of bigger foraminifera (Fig. 3E, 3F). The clay minerals accompanying such a microsparite inhibited its growth and could undergo glauconitization (Fig. 4G). The intergranular microsparite cement in samples No. 100 and 200 was developed in a similar way as in sample No. 300, whereas the clay matrix and micrite were dispersed mainly in intergranular pores (Fig. 4H).

The sparite cement was precipitated in the form of syntaxial overgrowths on fragments of echinoids (samples of varieties No. 100 and 200) (Fig. 4D), also infilling the fractures within these remains, with the thickness of the overgrowths reaching 20–40 μm. The plates and spines of echinoids were highly porous and very often dissolved and, in extreme cases, only their syntaxial rims remained. The microborings observed within the remains of echinoids were filled with glauconite or internal sediment, which underwent gradual glauconitization.

The mineralized zones, described above (section 3.1), were characterized by both an increased content of cement, and a reduced proportion of pores. The elongated skeletal remains observed within some of these zones were transversally fractured according to the course of such a zone, while in others, large bioclasts were arranged parallel to that direction, regardless of the main trend of the lineation in the sample.

2.3. Chemical and phase composition

The amount of acid-insoluble matter reached the value of ca. 10% for samples of varieties No. 100 and 200, whereas the residue of dissolution of the limestone variety No. 300 constituted only 1.45% of sample (Table 4). The majority of the insoluble substance of all the studied limestones was constituted of clay minerals and quartz as the XRD tests and SEM-EDS observations confirmed (Fig. 5). In X-ray patterns, diagnostic reflections of clay minerals clearly corresponded to the members of the smectite or mixed-layered illite-smectite group. Solvation with ethylene glycol changed the positions of their peaks, particularly for the basal spacing (001) (Fig. 6). There were also weak peaks in the X-ray pattern representing illit or/and muscovite, kaolinit and chlorite. Glauconite was found by SEM-EDS analysis (Fig. 4F). The minor components of the matrix were iron oxides/hydroxides and an organic substance.

Table 4. Content of selected chemical constituents in the samples of limestones from the Włochy deposit (according to the methods described in section 1.3)

Tabela 4. Zawartość wybranych składników chemicznych w próbach wapieni ze złoża Włochy (wg metodyki opisanej w rozdziale 1.3)

Content	Variety No. 100	Variety No. 200	Variety No. 300
Acid-insoluble matter [%]	10.22	10.59	1.45
Carbonaceous material [%]	0.29	0.27	0.21
Total LOI at 1000°C [%]	39.19	39.05	43.23
$CaCO_3$ [%] – estimated	ca. 88.5	ca. 88.2	ca. 97.8

The content of the latter did not exceed 0.3% in the varieties No. 100 and 200, and was ca. 0.2% in the variety No. 300 (Table 4). Moreover, the SEM-EDS tests also revealed the presence of sporadic grains of rutile and zircon.

The contents of calcium carbonate were estimated using the LOI results (at 1000°C) and the mass loss at 375°C associated with the loss of moisture and carbonaceous material (Table 5). The limestone variety No. 300 contained ca. 98% of calcium carbonate, while the proportion of that component was ca. 88% in the samples of other varieties. In the SEM observation, crystals of that mineral formed variable shapes and the smallest of them had the size measured in fractions of micron (Fig. 5A, 5B).

The dissolution of limestone aggregate of 2–5 mm fraction in water showed the highest solubility of calcium carbonate in the finest grained variety No. 200 (Table 5). The amount of Ca (18.06 mg/l), obtained in this case, after recalculation into $CaCO_3$, gave the solubility of calcium carbonate close to the possible maximum in the test conditions. Other elements also had the highest content in solutions of fine-grained limestone samples (varieties No. 100 and 200).

Table 5. Content of selected chemical constituents in water solutions of limestones from the Włochy deposit

Tabela 5. Zawartość wybranych składników chemicznych w wodnych roztworach wapieni ze złoża Włochy

Content	Variety No. 100	Variety No. 200	Variety No. 300
Ca [mg/l]	10.25	18.06	15.04
Si [mg/l]	3.10	4.00	2.26
Mg [mg/l]	1.04	1.17	1.12
Na [mg/l]	1.46	2.94	1.51
K [mg/l]	1.98	1.44	0.34
P [mg/l]	0.84	0.64	0.76
S [mg/l]	4.22	7.61	5.25

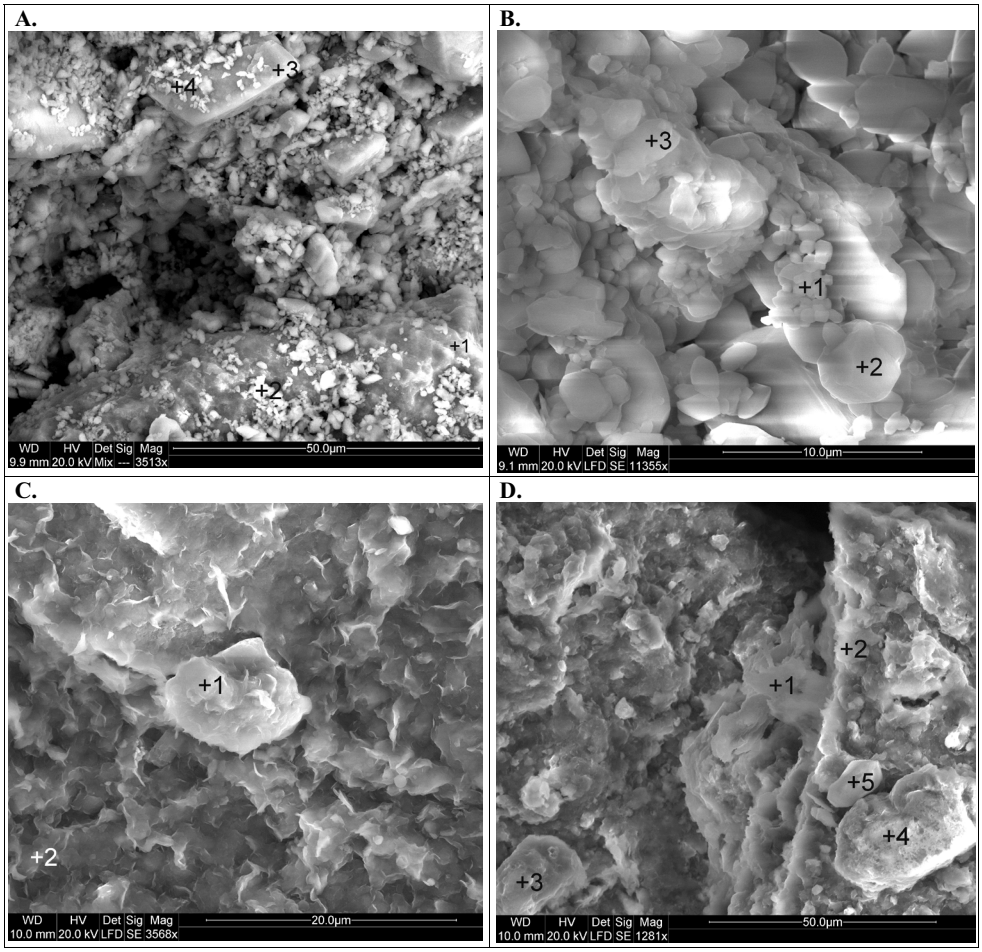

Fig. 5. Carbonate cements and clay matrix of the organodetrital limestones observed in rock fragments (A, B) and residuum of the acid solutions of limestones (C, D) with scanning electron microscope.
Photos by G. Stańczak.
The diversity of texture and shapes of calcium carbonate crystals: A – sample 200 (points 2, 3, 4) and B – sample 300 (points 1, 2). Large quartz grain in the lower part of image A (point 1) covered by micritic matrix (point 2). Clay matrix visible as fine flakes (point 3) in image B. The residuum of the filtered acid solutions of limestones: quartz grains (C – sample 200, point 1; D – sample 300, points 4, 5); flakes of clay minerals (C – point 2; D – points 1, 2, 3)

Rys. 5. Spoiwo węglanowe i matriks ilasta wapieni organodetrytycznych obserwowane w skaningowym mikroskopie elektronowym we fragmentach skał (A, B) i w pozostałości po rozpuszczeniu wapieni w kwasie (C, D). Fot. G. Stańczak.
Zróżnicowanie tektury i kształtu kryształów węglanu wapnia: A – próba 200 (punkty 2, 3, 4) i B – próba 300 (punkty 1, 2). Duże ziarno kwarcu w dolnej części zdjęcia A (punkt 1) pokryte przez mikrytową matriks (punkt 2). Matriks ilasta widoczna jako drobne łuski (punkt 3) na zdjęciu B. Pozostałość po rozpuszczeniu wapieni w kwasie: ziarna kwarcu (C – próba 200, punkt 1; D – próba 300, punkty 4, 5; łuski minerałów ilastych (C– punkt 2; D – punkty 1, 2, 3)

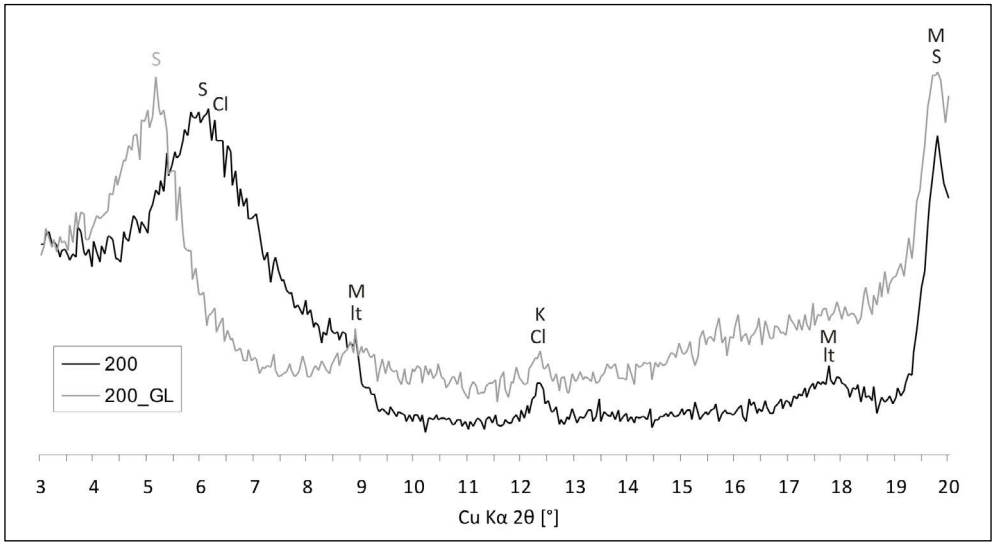

Fig. 6. X-ray diffraction patterns of untreated and glycolated (GL) samples of limestone variety No. 200. S – smectite or mixed-layered illite-smectite group, It – illite, M – muscovite, Cl – chlorite, K – kaolinite

Rys. 6. Dyfraktogramy rentgenowskie próbek surowych i nasyconych glikolem (GL) wapienia odmiany nr 200. S – minerały z grupy smektytu lub mieszanopakietowe z grupy illitu-smektytu, It – illit, M – muskowit, Cl – chloryt, K – kaolinit

The presence of some of them, i.e. Si, Mg, Na, K can be associated with clay matrix or the finest quartz fractions. High-Mg calcite and calcium sulphate can be components of the coralline algae (red algae) skeletons (Milliman 1974; Oti and Müller 1985), therefore, the dissolution of the biodetritus could be a source of Mg and S in solutions. The presence of this second element may be partly due to the dissolution of the gypsum and/or anhydrite present in the sulfate evaporative formations overlying the Pińczów Limestones in the Miocene profile (Łyczewska 1975, Alexandrowicz et al. 1982).

2.4. Physical properties

Among the most numerous samples of variety No. 100, the majority were characterized by the apparent density of 1.70–1.77 Mg/m^3 and water absorption by weight of 14.5–16.0%, and only some of them have the water absorption close to 18% and the low apparent density of 1.65–1.70 Mg/m^3 (Table 6). A significantly lower apparent density (ca. 1.60 Mg/m^3) and higher water absorption (over 20%) were found in fine-grained limestones of variety No. 200. The samples of variety No. 300, all cut from a small block of limestone, had the highest coefficients of variation of physical properties. Their average water absorption was similar to the samples of variety No. 100, but individual samples were characterized by water absorption in the range of 12.6–17.5%, while the apparent density of limestone of this

variety reached even 1.91 Mg/m^3. A large variability of the physical properties of variety No. 300 results from the large size and varied shapes of organic remains that build this limestone, and its poor sorting. The various content of bioclasts with intraparticle porosity and packing density of clastic material cause significant differences in the values of discussed parameters for samples collected from the same bed at a distance of several centimetres. The vertical and lateral variations in petrography were also found by Rajchel and Myszkowska (1998) in the Paleocenian red algal limestones from Bircza in the Skole Unit (Outer Eastern Carpathians) and by Bednarik et al. (2014) in the Badenian–Sarmatian limestones from Vienna and Styrian Basins, which were formed in a similar environmental regime.

A low apparent density of the studied rocks, called soft porous limestones, is due to a relatively high average total porosity, the value of which, depending on the research method, reached ca. 31–36% for varieties No. 100 and 300, and ca. 38–41% for variety No. 200 (Table 6, 7). These results were confirmed by the proportions of pores measured in microscopic analysis (Table 3). With the magnification available in the polarizing microscope, it was possible to observe only about quarter of them, among which the intergranular pores were of great importance, especially in the fine-grained limestones of variety No. 200.

Table 6. Physical properties of the limestones from the Włochy deposit according to the technical standards

Tabela 6. Właściwości fizyczne wapieni ze złoża Włochy wg norm technicznych

Physical parameter		Apparent density [Mg/m^3]	Water absorption [%]	Open porosity [%]	Total porosity* [%]	Water absorption coefficient by capillarity [g/m^{2}s^{0,5}]
Method of test		PN-EN 1936	PN-EN 13755	PN-EN 1936	PN-EN 1936	PN-EN 1925
Variety No. 100	mean	1.72	15.56	26.77	36.25	332.57
	range	1.65–1.77	14.49–17.68	25.53–29.17	34.52–38.88	212.48–416.89
	c.v.	1.40	4.26	2.85	2.47	14.14
	n	103	103	103	103	37
Variety No. 200	mean	1.60	21.07	33.75	40.67	377.93
	range	1.59–1.61	20.39–21.82	32.71–34.69	40.34–41.11	–
	c.v.	0.55	3.51	3.08	0.80	–
	n	4	4	4	4	1
Variety No. 300	mean	1.77	15.74	27.78	34.35	307.58
	range	1.71–1.91	12.60–17.50	24.09–29.91	29.21–36.72	170.52–372.28
	c.v.	4.13	11.20	7.63	7.89	23.34
	n	8	8	8	8	6

* According to Przybyszewski (2007) the specific density of limestones equal to 2.72 Mg/m^3 was accepted in the porosity calculations, n – No. of tested specimens, c.v. – coefficient of variation [%].

Table 7. Parameters of the limestones from the Włochy deposit derived from mercury porosimetry

Table 7. Właściwości wapieni ze złoża Włochy uzyskane na podstawie porozymetrii rtęciowej

Parameter	Bulk density [Mg/m^3]	Total interparticle porosity >350 nm [%]	Total intraparticle porosity <350 nm [%]	Total porosity [%]	Content of supercapillary pores >100 µm [%]	Content of capillary pores 0.2–100 µm [%]	Content of subcapillary pores <0.2 µm [%]
					Σ = 100%		
Variety No. 100	1.71	30.23	1.59	31.82	2.54	93.78	3.68
Variety No. 200	1.59	36.70	1.30	37.99	1.40	95.79	2.81
Variety No. 300	1.78	31.09	1.94	33.04	4.09	92.11	3.80

The pore system in majority is built by open pores communicated with each other, which are available for water at atmospheric pressure, particularly in samples of variety No. 200 (average open porosity ca. 34%) (Table 6). In the porosimetry tests (Table 7) ca. 92.1–95.8% of all the pores, being available for mercury, represented capillary pores with diameters of 0.2–100 µm (the highest percentage for variety No. 200), and 2.8%–3.8% constituted subcapillary pores with smaller diameters of throats (classification of pores by Plewa and Plewa 1992). Limestone of variety No. 300 was distinguished by the highest proportion of supercapillary pores. The discrepancy in the values of total porosity obtained in porosimetry tests and the one calculated on the basis of apparent and specific densities of limestones suggests that a few percent of all pores can be unavailable for liquids.

The analysis of the capillary rise of water enabled one to conclude that for all tested varieties of limestone from the Włochy deposit the water absorption coefficient by capillarity was high and was within the range of 170–417 g/m^{2}s$^{0.5}$, and for most samples within 300–400 g/m^{2}s$^{0.5}$ (Table 6). This parameter is weakly negatively correlated with the apparent density (R^2 = 0.55) (Fig. 7), and thus depends on the sizes of the pores and their proportions in the rock, which, as shown in the test results described above, belonged in majority to the capillary pores. The lowest water absorption coefficient by capillarity characterized all the samples of limestone variety No. 300 (170–373 g/m^{2}s$^{0.5}$) and selected samples of variety No. 100, in which the zones of mineralization have been identified (212–286 g/m^{2}s$^{0.5}$). In the former, it could be the consequence of the presence of supracapillary pores and in the latter the zones of calcification, preventing the capillary movement of water.

Samples with the highest coefficient of water absorption by capillarity reached approx. 98% of its maximum mass in the state of saturation in about 30 minutes, while those with the lowest coefficient – in about 2–3 h. The tests of capillary action were additionally carried out for two limestone samples of variety No. 100, in 30-centimeter beams with a base

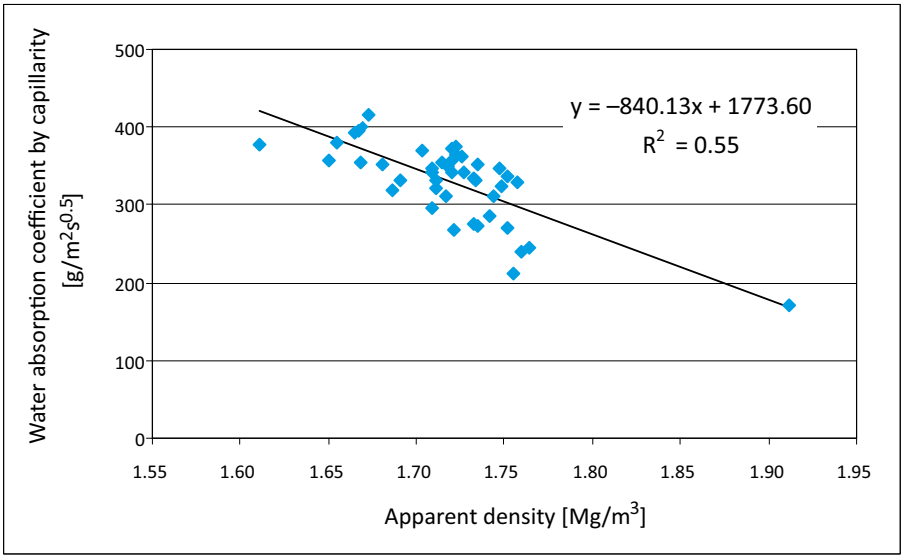

Fig. 7. Relation between apparent density and capillary water absorption for the samples of limestones from the Włochy deposit

Rys. 7. Zależność pomiędzy gęstością pozorną a nasiąkliwością kapilarną dla próbek wapieni ze złoża Włochy

of 50 × 50 mm, showed that in the first 15 minutes of this process, the water saturated the sample at a rate of ca. 0.16 cm/min. The rate of capillary action quickly decreased through the time and after 1 hour it was ca. 0.05 cm/min, and in the final phase of the test, after 41 hours only ca. 0.004 cm/min. According to the obtained relationship between the time and the height of the water rise:

$$y = -0.007x^2 + 0.936x - 1.037 \; [R^2 = 0.999] \quad (1)$$

where:
- x – a square root of time [$min^{0.5}$],
- y – a height of water rise [cm], it can be predicted that capillary water would reach a maximum height of ca. 33 cm after 86 hours, gaining a state of balance between surface tension, gravity and evaporation.

In order to investigate the influence of the rock structure (fabric) on the water absorption by capillarity, samples of variety No. 100 of the narrow range of water absorption (15–16%) were divided into three groups, in which different sides (A, B or C, respectively) were immersed. The results obtained indicated that the intensities of capillary pore saturation were similar regardless of the direction of that process (351 $g/m^2s^{0.5}$, 345 $g/m^2s^{0.5}$ and 347 $g/m^2s^{0.5}$, respectively) and the arrangement of the pore connections had little impact on that parameter.

2.5. Mechanical properties

The measurements of the longitudinal ultrasonic waves velocity (V_L) were performed to investigate the connections between the microstructure and elastic properties of limestones. The results of the research carried out has shown that the value of these parameter is strictly dependent on the size of the grains as well as the dimensions and distributions of pore spaces.

The highest ultrasonic waves velocity (average values of 3.15 km/s) was reached for the dried samples of the coarse-grained limestones of variety No. 300, while the lowest value of these parameter was registered for the fine-grained limestones of variety No. 200 (2.38 km/s) (Table 8). The relatively high values of the ultrasonic wave velocity were noted in the samples in which macroscopically visible mineralized zones of calcification occurred.

The high coefficient ($R^2 = 0.79$) of correlation between the velocities of ultrasonic waves measured in dry samples of limestones and their apparent densities implies that the main factor affecting the pulse course through a sample is the network of pores. The effective transmission of vibrations in samples of variety No. 300 is provided by the rigid skeleton built of numerous large bioclasts (mainly red algae, bryozoans and foraminifera) bonded with the sparite cement prevailing on matrix, all of them constituting 90.9% of the rock volume in total. This is also favoured by the least-developed pore space (the relatively small total porosity and the highest amount of the supercapillary pores) (Table 6, 7). In contrast, the numerous pores, especially the intergranular ones existing between small particles, and the disintegrated structure of red algae fragments, limit the transfer of the ultrasonic pulse in the limestones of variety No. 200 (Fig. 3C, 3D).

The influence of water saturation on the ultrasonic wave velocity was tested for the samples of limestone, and otherwise as it was expected (Bromowicz and Figarska-Warchoł 2010; Török and Vásárhelyi 2010), the water saturation decreased the ultrasonic wave velocity (on average by 0.27 km/s, 0.30 km/s and 0.04 km/s for the samples of varieties nos. 100, 200 and 300, respectively). The lower values of the dry-state ultrasonic wave velocity, the higher the decrease of the wet-state velocities ($R^2 = 0.60$) (Fig. 8). The water saturation of the studied samples probably induces swelling and plasticization of the clay matrix, as well as the partial dissolution of the finest carbonate fractions, and, in consequence, weakens the connections between detrital components in the rock skeleton.

The very high correlation between velocities of the ultrasonic wave obtained for dry and saturated samples ($R^2 = 0.96$) gives the opportunity to predict the latter parameter without the need of measurements on samples in different states. That relation can be represented by the equation:

$$y = 1.29x - 1.04 \tag{2}$$

where:
- x – an ultrasonic wave velocity measured in dry sample,
- y – an ultrasonic wave velocity measured in the wet sample.

Table 8. Mechanical properties of the limestones from the Włochy deposit

Tabela 8. Właściwości mechaniczne wapieni ze złoża Włochy

Variety	Statistical parameter	Longitudinal ultrasonic wave velocity [km/s] perpendicular to the surface:					
		A	B	C	A	B	C
		in the dry state			in the water-saturated state		
Variety No. 100	mean	2.69			2.43		
		2.70	2.68	2.70	2.43	2.41	2.45
	range	2.44–2.95	2.46–2.90	2.50–2.99	2.08–2.68	2.10–2.61	2.19–2.72
	n	52	52	52	52	52	52
Variety No. 200	mean	2.38			2.08		
		2.36	2.38	2.28	2.11	2.05	1.89
	range	2.33–2.41	2.30–2.43	2.28–2.29	2.01–2.19	1.96–2.15	1.88–1.90
	n	3	3	2	3	3	2
Variety No. 300	mean	3.15			3.11		
		3.13	3.12	3.20	3.09	3.10	3.14
	range	2.85–3.60	2.73–3.72	3.00–3.95	2.76–3.61	2.75–3.76	2.91–3.87
	n	6	6	6	6	6	6
	Statistical parameter	Uniaxial compressive strength [MPa] perpendicular to the surface:					
		A	B	C	A	B	C
		in the dry state			in the water-saturated state		
Variety No. 100	mean	12.20			7.36		
		11.30	10.57	13.47	6.58	6.80	8.02
	range	7.88–14.07	9.63–11.43	11.19–14.97	5.48–7.81	4.64–8.31	5.58–10.88
	n	3	3	6	3	3	6

n – number of specimens.

The results of velocities of the ultrasonic pulse measured in directions parallel to the bedding (A and B) for all the samples revealed that none of them were privileged. In turn, the wave velocities tested perpendicular to the bedding (C) in samples of varieties No. 100 and 300, were slightly higher than the average velocity in directions A and B and the difference did not exceed 75 m/s. That relation concerned various textural varieties (fine- and coarse-grained) of both dry and water saturated samples. The anisotropy coefficient calculated for dry samples was within the limits of 1.01–1.04, and for saturated ones in the range of 1.02–1.17. These values are similar to the results obtained for the Pińczów Limestones

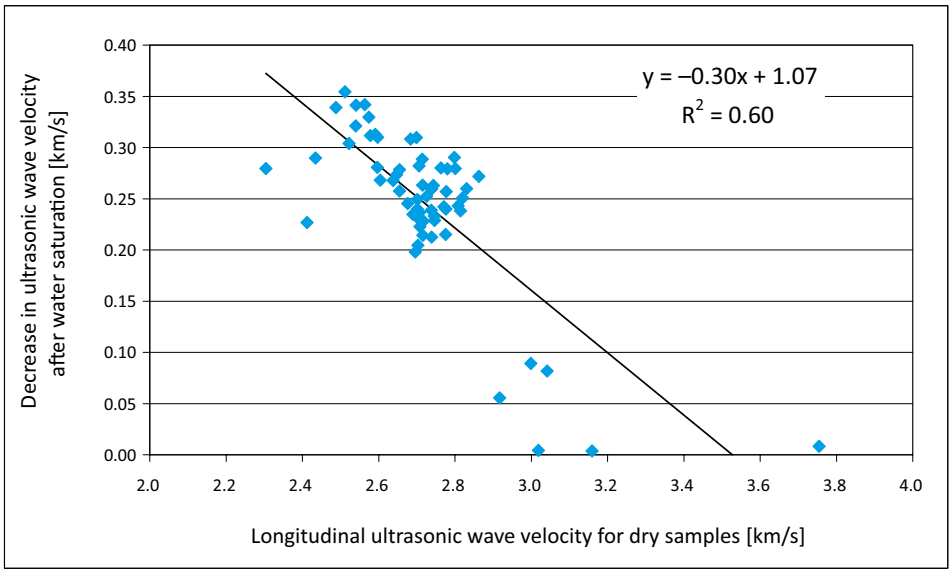

Fig. 8. Relation between longitudinal ultrasonic wave velocity for dry samples of limestones and its decrease after water saturation (variety No. 100)

Rys. 8. Zależność pomiędzy prędkością podłużnych fal ultradźwiękowych suchych wapieni a jej spadkiem po nasyceniu prób wodą (odmiana nr 100)

by Pinińska ed. (1994) – 1.03 and 1.06, respectively, and show a generally low anisotropy of the discussed parameter. This may be due to poor sorting and a low degree of spatial arrangement of organic skeletons, which are the main path of the sound pulse transition, all the more so that the structure of the major biodetrital components, i.e. red algae or bryozoans, is a complex and highly porous.

The selected samples of variety No. 100 were subjected to the uniaxial compressive strength tests (UCS). Dried samples were characterized by low compressive strength within the range of 7.9–15.0 MPa (Table 8). The saturation of the samples with water caused the reduction in strength by 3.8–5.5 MPa, which constituted ca. 36–42% of this parameter value for samples in the dry state. There was no essential difference of this parameter in respect to the direction of force acting in the planes parallel to the bedding (UCS_A or UCS_B), while the strength against the load applied perpendicular to the bedding (UCS_C) was higher than the ones measured in other directions by ca.1.3 MPa for dry, and by ca. 2.5 MPa for saturated samples. The reason for this may be the observed directional orientation of some of the elongated and flat grains as it was previous revealed for granitoids by Přikryl (2001). The anisotropy coefficient of the discussed parameter was 1.27 and 1.23 in dry and water-saturated conditions, respectively. The reduction of the anisotropy of wet samples results from the aforementioned changes of clay matrix and micrite (swelling, dissolution), causing the plasticization of samples observed during the tests.

The relation ($R^2 = 0.69$) between the uniaxial compressive strength (UCS) and the velocity of longitudinal wave (VL) was found for samples tested in the same direction regardless of their state (Fig. 9). The water saturation had a smaller effect on the compressive strength reduction in the case of samples characterized by better elastic properties (higher velocities of the ultrasonic wave). The linear model of that relationship was described by the following equation:

$$y = 14.02x - 25.82 \tag{3}$$

- x – an ultrasonic wave velocity (V_L),
- y – a uniaxial compressive strength (UCS), both measured in the same direction. The mean absolute percentage error was equal to 14.2% when the above equation (3) was applied to estimate the values of latter parameter (UCS).

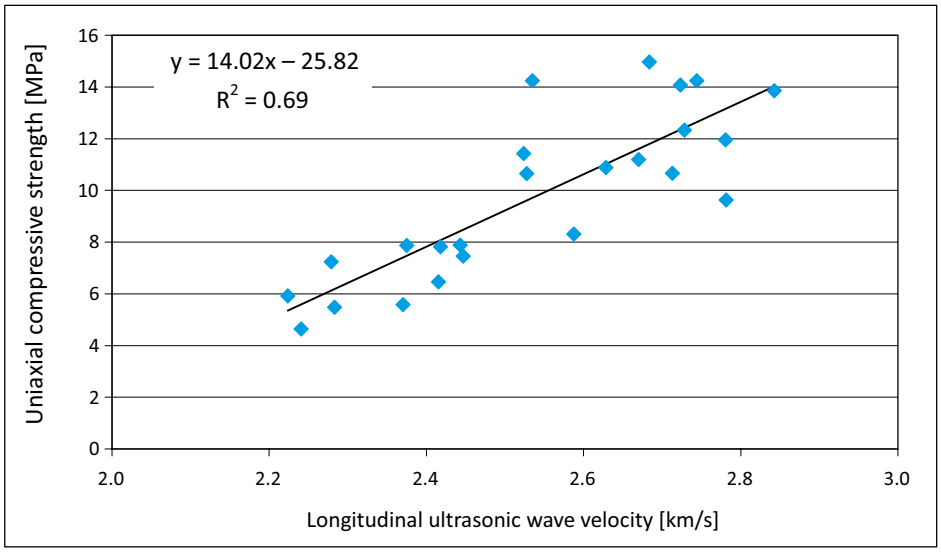

Fig. 9. Relation between longitudinal ultrasonic wave velocity and uniaxial compressive strength, both tested in the same direction, for dry and water saturated samples of limestones from the Włochy deposit (variety No. 100)

Rys. 9. Zależność pomiędzy prędkością podłużnych fal ultradźwiękowych a wytrzymałością na jednoosiowe ściskanie, w obu przypadkach badanych w tym samym kierunku, dla suchych i nasyconych wodą prób wapieni ze złoża Włochy (odmiana nr 100)

It was estimated that the UCS values for the dry samples of variety No. 100 should be ca. 8.4–14.0 MPa, while laboratory tests yielded results in the range of 7.9–15.0 MPa. In the case of water-saturated samples, the values of this parameter were estimated at 5.3–11.0 MPa, and 5.5–10.9 MPa were obtained in tests, and these laboratory results were more strongly correlated with the expected values ($R^2 = 0.70$) than in the case of dry samples ($R^2 = 0.13$)

The confirmed relationship between the V_L and UCS values (equation 3) gave the ability to predict the latter parameter of value below 5 MPa for the water-saturated samples of variety No. 200, while for most samples of variety No. 300 within the range of 13–28 MPa.

2.6. The comparison of studied rock varieties to other Leitha Limestones

The data provided in publications gave the possibility to compare the obtained results with the quality of the Pińczów Limestones cropping out in the vicinity of the Włochy deposit (Penkalowa 1963; Dębski 1966; Bugajska-Pająk 1974; Rutkowski 1980; Kozłowski 1986; Pinińska 1994). The values of apparent density, water absorption and uniaxial compressive strength of the analysed samples were within the limits given for the Pińczów, Skowronno and Bogucice-Zakamień deposits. For limestones from these quarries, the relation between texture and strength resistance (the finer grained the lower UCS values) was also stated. Moreover, the decrease of those parameter values after water saturation were in the range 25–47% and this corresponded to the results obtained in the studies. The similar results of physical properties were also reported for the Pińczów Limestones used in Krakow monuments by Haber et al. (1991), who stated that the type of coarse-grained limestones, containing the smallest quantities of micrite and clay matrix, revealed the highest weathering resistance.

The quality comparison of the examined limestones and porous limestones from other European locations led to the conclusion that the values of geotechnical properties of shallow marine carbonates of the Miocene age often fall into the same ranges (Török 2003; Török et al. 2004; Laho et al. 2010; Bögöly 2015; Pappalardo et al. 2016; Baud et al. 2017; Festa et al. 2018). However, differences in their detail petrographic characteristics can influence on the exact values of the mechanical parameters. Thus, one can find the resemblance between the coarse-grained limestones of variety No. 300 and Leitha Limestones from Winden (Vienna Basin) and Roemersteinbruch St. Margarethen (the transition zone between the Eisenstadt–Sopron Basin and the Danube Basin) quarries described as coarse grained coralline–algal–bryozoan–echinoderm packstones (Bednarik 2014). Moreover, the fine-grained samples of variety No. 200 have physico-mechanical properties similar to very porous and weakly cemented, detrital limestones from the Aflenz Roman quarry (Styrian Basin) formed as carbonatic-siliciclastic packstone with highly fractured bioclasts (Bednarik 2014). The fabric and petrophysical properties of the limestones of variety No. 100 are close to the bioclastic limestone from the Fertőrákos quarry (Eisenstadt–Sopron Basin) which contains major amount of red algae fragment, forams and small intraclasts (Pápay and Török 2017).

Conclusions

The research carried out showed that in the Włochy deposit – the only Pińczów Limestone deposit being currently exploited – there are various textural varieties of the organodetrital

www.czasopisma.pan.pl PAN POLSKA AKADEMIA NAUK www.journals.pan.pl

facies of red algal limestones: from the fine-grained, found in the lower part of the south wall of the excavation (variety No. 200) to the coarse-grained (variety No. 300) whose samples were taken from the upper part of the profile. Nowadays, the subject of particular interest of the quarry operator are limestones on the verge of fine- and medium-grained (variety No. 100), which comes from the lower layer of the deposit with more opportunities of extracting large stone blocks. All varieties of limestones are constituted of poorly or moderately sorted skeletal remains, dominated by red algae, bryozoans and foraminifera and preserved in different stages, that are bonded with sparite cement, micrite and clay matrix.

Limestone variety No. 300, coarse-grained and poorly sorted, consists mainly of well-preserved red algae and large-sized bryozoans with numerous large pores (up to 0.6 mm in diameter), connected by narrower throats, filled with sparite cement to varying degrees (in total 15.2% of volume) and, more rarely, micrite and clay matrix (in total 8.4% of the volume). Microscopic measurements revealed a relatively little amount of pores (9.1% counted in thin section, 34.35% in technical studies according to standards, 33.04% in the porosimeter test) that is constituted of intragranular pores merely in half. This is connected to the comparatively low water absorption at atmospheric pressure (15.74%) and by the capillarity (307.58 $g/m^2s^{0.5}$) of these limestones. Large-sized organic debris bonded together with cement and matrix (constituting a total of 90.9% of the rock volume), guarantee a relatively fast transmission of the ultrasonic wave through a rigid framework of rock (3.15 km/s). The above physical and technical parameters indicate that discussed variety is most useful as a building material.

While in the samples of variety No. 300, the structure of red algae is compact, additionally reinforced with cement, in the fine-grained limestone of variety No. 200 fragments of these components are porous and disintegrated. In the latter variety, the most important organic remains are foraminifera, mainly their small or crushed forms. Bryozoans in fine-grained varieties No. 100 and 200 are minor constituents, whereas the detrital grains, such as quartz, are present in significant content. The sparite cement forms rims around individual organic debris or builds up on their internal walls, but often does not bond the grains together. The intergranular spaces are filled with matrix or remain empty, making the limestone of variety No. 200 the most porous (13.9% counted in thin section, 40.67% in technical studies according to standards, 37.99% in the porosimeter test) with the largest amount of well-communicated intergranular pores (approx. 83% of all pores). As a consequence, the samples of this variety are characterized not only by the highest water absorption (21.07%) and capillary water absorption coefficient (377.93 $g/m^2s^{0.5}$), but also the lowest values of the ultrasonic waves velocity (2.38 km/s), additionally reduced by approx. 0.27 km/s after water saturation, which may result from dissolving the finest carbonate particles and swelling of clay minerals belonging to the smectite or mixed-layered illite-smectite group. The role of the amount and morphology of micrite crystals and their manner of filling the pore space concerning the acoustic properties of porous limestones was described by Regnet et al. (2015).

The characteristics of lithofacies distinguished within the studied limestones of the Badenian Pińczów formation and their comparison to the described ones in the Leitha Limestones

www.czasopisma.pan.pl PAN POLSKA AKADEMIA NAUK www.journals.pan.pl

from the Viena Basin allow to assume that their sedimentary environment was connected with algal-bryozoan reefoidal structures developed in the shallow-marine shoal (Riegl and Piller 2000; Górka 2002; Wiedl et al. 2012). Limestones of variety No. 300 represent facies that were formed in the zone of higher energy (coarser grains, poorer sorting, chaotic arrangement of components) where the supply of terrigenous material was limited. On the other hand, the features of variety No. 100 and especially No. 200 (finer grains, better sorting, linear arrangement of larger remains and presence of lamination) indicate that they formed in the deeper environment. The vertical succession of these varieties (from the bottom, varieties No. 200, 100 and 300) suggests that the depth in sedimentary basin could diminish.

The effects of diagenetic processes, such as calcite cementation filling pores, are manifested in the studied limestone by an increase of the apparent density and more intensive lithification, also observed by other authors (Rutkowski 1976; Dullo 1983). Tectonic phenomena affecting the discussed formations caused the development of stress surfaces along which the detrital grains were displaced or fractured depending on the concurrent degree of sediment consolidation. They were also associated with the crystallization of calcium carbonate, now evidenced in the form of mineralized zones. Their occurrence in the rock improves its physical and mechanical properties.

The described variability of physical and mechanical properties in the profile of deposit (samples taken from different beds), as well as within a single bed (variability of parameters for samples cut out from one block), forces one to make current petrographic observations and laboratory tests during the exploitation process to omit the parts of rock mass with the worse quality parameters. The relationships found between the properties can be helpful here. Estimation of strength parameters can be carried out basing on non-destructive tests, i.e. the determination of water absorption, apparent density or ultrasonic waves velocity (Török 2003; Bögöly et al. 2015).

Comparison of the obtained results with the properties of the Leitha Limestones from other deposits shows that their quality is similar. Therefore, as in many previous examples of applications, they can be used as facing or sculptural stone because of their appropriate parameters. This is supported by low apparent density and good insulation properties due to their high porosity. On the other hand, the high absorbability of limestones limits the possibilities of their use for the interiors or forces the user to apply the impregnants. However, the relatively poor arrangement of grains and the low anisotropy of the properties enable one to select the direction of stone processing without constrains.

Acknowledgements

The authors would like to thank the Reviewers for their in-depth analysis of the manuscript and important remarks, and Mr. Jacek Łata for providing geological documentation and substantial help in the preparation of the samples.

This work was financially supported by the AGH University of Science and Technology statutory grant No. 11.11.140.161 and subsidy of the Polish Ministry of Science and Higher Education No. 16.16.140.315.

www.czasopisma.pan.pl PAN POLSKA AKADEMIA NAUK www.journals.pan.pl

REFERENCES

Adams, A.E. and Mackenzie, W.S. 2011. *Carbonate sediments and rocks under the microscope: a colour atlas*. Manson Publishing, London.

Adams et al. 1991 – Adams, A.E., Mackenzie, W.S. and Guilford, C. 1991. *Atlas of sedimentary rocks under the microscope*. Longman House, Burnt Mill, Harlow.

Alexandrowicz et al. 1982 – Alexandrowicz, S.W., Garlicki, A. and Rutkowski, J. 1982. Basic lithostratigraphic units of the Miocene in the Carpathian Foredeep (*Podstawowe jednostki litostratygraficzne miocenu zapadliska przedkarpackiego*). *Kwartalnik Geologiczny* 26, 2, pp. 470–471 (*in Polish*).

Areń, B. 1971. Tertiary of the Świętokrzyskie region (*Trzeciorzęd regionu świętokrzyskiego*). *Prace Instytutu Geologicznego* 64, pp. 107–121 (*in Polish*).

Bathurst, R.G.C. 1975. Carbonate sediments and their diagenesis. *Developments in Sedimentology* 12. Elsevier Publishing Company, Amsterdam–London–New York.

Baud et al. 2017 – Baud, P., Exner, U., Lommatzsch. M., Reuschle, T. and Wong, T. 2017. Mechanical behavior, failure mode, and transport properties in a porous carbonate. *Journal of Geophysical Research: Solid Earch* 122(9), pp. 7363–7387.

Bednarik et al. 2014 – Bednarik, M., Moshammer, B., Heinrich, M., Holzer, R., Laho, M., Rabeder, J., Uhlir, C. and Unterwurzacher, M. 2014. Engineering geological properties of Leitha Limestone from historical quarries in Burgenland and Styria, Austria. *Engineering Geology* 176, pp. 66–78.

Bögöly et al. 2015 – Bögöly, G., Török, Á. and Görög, P. 2015. Dimension stones of the North Hungarian masonry arch bridges. *Central European Geology* 58, 3, pp. 230–245.

Bromowicz, J. 1974. Facial variation and lithological education of the inoceram sandstone of the Skole unit between Rzeszów and Przemyśl (Zmienność facjalna i wykształcenie litologiczne piaskowców inoceramowych jednostki skolskiej między Rzeszowem a Przemyślem). *Prace Geologiczne Komisji Nauk Geologicznych PAN, Oddział w Krakowie* 84, pp. 1–83 (*in Polish*).

Bromowicz et al. 2004 – Bromowicz, J., Figarska-Warchoł, B., Karwacki, A., Kolasa, A., Magiera, J., Rembiś, M., Smoleńska, A. and Stańczak, G. 2004. Evaluation of the deposits of building and road stones -various points of view (*Waloryzacja złóż kamieni budowlanych i drogowych z różnych punktów widzenia*). *Prace Naukowe Instytutu Górnictwa Politechniki Wrocławskiej* 108. *Seria: Konferencje* 40, pp. 3–11 (*in Polish*).

Bromowicz et al. 2005 – Bromowicz, J. ed., Figarska-Warchoł, B., Karwacki, A., Kolasa, A., Magiera, J., Rembiś, M., Smoleńska, A. and Stańczak, G. 2005. Valorisation of Polish deposits of building and road stones against the background of European Union regulations (*Waloryzacja polskich złóż kamieni budowlanych i drogowych na tle przepisów Unii Europejskiej*). Kraków: Uczelniane Wydawnictwa Naukowo-Dydaktyczne AGH (*in Polish*).

Bromowicz, J. and Figarska-Warchoł, B. 2010. Report on the investigations of rocks changes caused by freezing (*Raport z badań nad zmianami właściwości skał wywołanych zamrozem*). *Prace Naukowe Instytutu Górnictwa Politechniki Wrocławskiej* 130. *Studia i Materiały* 37, pp. 41–55 (*in Polish*).

Bromowicz, J. and Figarska-Warchoł, B. 2012. Decorative and architectural stones in south-eastern Poland – the deposits, their resources and perspectives of exploitation (*Kamienie dekoracyjne i architektoniczne południowo-wschodniej Polski – złoża, zasoby i perspektywy eksploatacji*). *Gospodarka Surowcami Mineralnymi – Mineral Resources Management* 28, pp. 5–22 (*in Polish*).

Bugajska-Pająk, A. 1974. Raw material characteristic of light limestones from the miocene of southern margin of the Holy Cross Mts (*Charakterystyka surowcowa wapieni lekkich miocenu południowego obrzeżenia Gór Świętokrzyskich*). *Przegląd Geologiczny* 257 (9), pp. 416–421 (*in Polish*).

Dębski, W. ed. 1966. Monograph on stone deposits in Poland. South-central Poland (*Monografia złóż materiałów kamiennych w Polsce. Okręg południowo-centralny Polski*). COBiRTD, Warszawa (*in Polish*).

Doláková, N., Brzobohatý, R., Hladilová, Š. and Nehyba, S. 2008. The red-algal fades of the Lower Badenian limestones of the Carpathian Foredeep in Moravia (Czech Republic). *Geologica Carpathica* 59, 2, pp. 133–146.

Drewniak, A. 1994. Coralline algae from the Pińczów Limestones (Middle Miocene; southern slopes of the Holy Cross Mountains, Central Poland) as environmental indicators. *Acta Geologica Polonica* 44, 1–2, pp. 117–135.

www.czasopisma.pan.pl PAN POLSKA AKADEMIA NAUK www.journals.pan.pl

Dullo, W.C. 1983. Fossildiagenese im miozänen Leitha-Kalk der Paratethys von Österreich: Ein Beispiel für Faunenverschiebungen durch Diageneseunterschiede. *Facies* 8, pp. 1–112.

Dunham, R.J. 1962. Classification of carbonate rocks according to depositional texture. *Amer. Ass. Petrol. Geol. Mem.* 1, pp. 108–121.

Embry, A.F. and Klovan, J.E. 1971. A late Devonian reef tract on northeastern Banks Island Nordwest Territories. *Bull. Canad. Petrol. Geol.* 19, pp. 730–781.

Festa et al. 2018 – Festa, V., Fiore, A., Luisi, M., Miccoli, M.N. and Spalluto, L. 2018. Petrographic features influencing basic geotechnical parameters of carbonate soft rocks from Apulia (southern Italy). *Engineering Geology* 233, pp. 76–97.

Figarska-Warchoł, B. and Stańczak, G. 2016. The effect of petrographic diversity of the Krosno Sandstones on their physico-mechanical properties in the Górka-Mucharz and Skawce deposits (Beskid Mały Mountains) (*Wpływ petrograficznego zróżnicowania piaskowców krośnieńskich na ich właściwości fizyczno-mechaniczne w złożach Górka-Mucharz i Skawce (Beskid Mały)*). *Zeszyty Naukowe Instytutu Gospodarki Surowcami Mineralnymi PAN* 96, 3, pp. 7–55 (*in Polish*).

Fijałkowska, E. and Fijałkowski, J. 1966. On the application of the Pińczów stone in early medieval buildings (*O zastosowaniu kamienia pińczowskiego w budowlach wczesnego średniowiecza*). *Przegląd Geologiczny* 14, 12, pp. 531–532 (*in Polish*).

Flügel, E. 2004. *Microfacies of Carbonate Rocks. Analysis, Interpretation and Application*. Springer-Verlag, Berlin Heidelberg.

Folk, R.L. and Ward, W.C. 1957. Brazos River bar: a study in the significance of grain size parameters. *Journal of Sedimentary Petrology* 27, 1, pp. 3–26.

Gadomski, J. 1970. Early Gothic sculpture of Madonna and Child in Wiślica (*Wczesnogotycka rzeźba Madonny z Dzieciątkiem w Wiślicy*). *Rocznik Muzeum Świętokrzyskiego* 6, pp. 161–185 (*in Polish*).

Górka, M. 2002. The Lower Badenian (Middle Miocene) coral patch reef at Grobie (southern slopes of the Holy Cross Mountains, Central Poland), its origin, development and demise. *Acta Geologica Polonica* 52, 4, pp. 521–534.

Haber et al. 1991 – Haber, J., Kozłowski, R. and Magiera, J. 1991. Destruction of Pińczów limestone in the monuments of Krakow (*Niszczenie wapienia pińczowskiego w zabytkach Krakowa*). *Rocznik Krakowski* 57, pp. 165–191 (*in Polish*).

Jasionowski, M. 1997. Outline of lithostratigraphy of Miocene deposits in the eastern part of the Carpathian Foredeep (*Zarys litostratygrafii osadów mioceńskich wschodniej części zapadliska przedkarpackiego*). *Biuletyn PIG* 375, pp. 43–60 (*in Polish*).

Jiménes-Moreno et al. 2006 – Jiménes-Moreno, G., Head, M.J. and Harzhauser, M. 2006. Early and Middle Miocene dinoflagellate cyst stratigraphy of the Central Paratethys, Central Europe. *Journal of Micropalaeontology* 25, pp. 113–139.

Jurkiewicz, H. and Woiński, J. 1979. Geological Map of Poland on a scale of 1: 200000. Sheet of Tarnów. Map without Quaternary tracks (*Mapa Geologiczna Polski w skali 1:200000. Arkusz Tarnów. Mapa bez utworów czwartorzędowych*). Warszawa: Wyd. Geologiczne (*in Polish*).

Kardyś, P. 2006. Wiślica in the Middle Ages and in the early modern period. Studies in the history of the city (*Wiślica w średniowieczu i w okresie wczesnonowożytnym. Studia z dziejów miasta*). Kielce: Kieleckie Towarzystwo Naukowe (*in Polish*).

Keeling, P.S. 1962. Some experiments on the low-temperature removal of carbonaceous material from clays. *Clay Minerals Bulletin* 28, pp. 155–158.

Kováč et al. 2007 – Kováč, M., Andreyeva-Grigorovich, A., Bajraktarević, Z., Brzobohatý, R., Filipescu, S., Fodor, L., Harzhauser, M., Nagymarosy, A., Oszczypko, N., Pavelić, D., Rögl, F., Saftić, B., Sliva, Ľ. and Studencka, B. 2007. Badenian evolution of the Central Paratethys Sea: paleogeography, climate and eustatic sea-level changes. *Geologica Carpathica* 58, 6, pp. 579–606.

Kowalewski, K. 1958. Miocene stratigraphy of southern Poland, with particular emphasis on the southern oblique of the Świętokrzyskie Mountains (Stratygrafia miocenu południowej Polski ze szczególnym uwzględnieniem południowego obrzeżenia Gór Świętokrzyskich). *Kwartalnik Geologiczny* 2, pp. 3–43 (*in Polish*).

Kozłowski, S. 1986. Rock raw materials of Poland (*Surowce skalne Polski*). Warszawa: Wydawnictwa Geologiczne (*in Polish*).

Krach, W. 1962. Outline of the stratigraphy of southern Poland (*Zarys stratygrafii Polski południowej*). *Rocznik PTG* 32, 4, pp. 529–557 (*in Polish*).

Laho et al. 2010 – Laho, M., Franzen, C., Holzer, R. and Mirwald, P.W. 2010. Pore and hyhric properties of porous limestones: a case study from Bratislava, Slovakia, in: Přikryl, R., Török, Á. eds. Natural Stone Resources for Historical Monuments. *Geological Society, London, Special Publications* 333, 1, pp. 165–174.

Łyczewska, J. 1971. Explanations to the Detailed Geological Map of Poland 1:50 000. Sheet of Jędrzejów (*Objaśnienia do Szczegółowej Mapy Geologicznej Polski 1:50 000. Arkusz Jędrzejów*). Warszawa: Wydawnictwa Geologiczne (*in Polish*).

Łyczewska, J. 1972. Explanations to the Detailed Geological Map of Poland 1:50 000. Sheet of Busko Zdrój (*Objaśnienia do Szczegółowej Mapy Geologicznej Polski 1:50 000. Arkusz Busko Zdrój*). Warszawa: Wydawnictwa Geologiczne (*in Polish*).

Łyczewska, J. 1975. Outline of the geological structure of the wójczo-pińczowski band (*Zarys budowy geologicznej pasma wójczo-pińczowskiego*). *Biuletyn Instytutu Geologicznego* 283, pp. 151–188 (*in Polish*).

Milliman, J.D. 1974. *Marine Carbonates* [In:] Milliman, J.D., Müller, G., Förstner, U. eds. *Recent Sedimentary Carbonates*. Springer-Verlag, Berlin – Heidelberg – New York.

Oti, M. and Müller, G. 1985. Textural and mineralogical changes in coralline algae during meteoric diagenesis: an experimental approach. *N. Jb. Geol. Paläont. Abh.* 151, pp. 163–195.

Pápay, Z. and Török, Á. 2017. Effect of Thermal and Freeze-thaw Stress on the Mechanical Properties of Porous Limestone. *Periodica Polytechnica Civil Engineering* [S.l.]. ISSN 1587-3773. [Online] https://pp.bme.hu/ci/article/view/11100 [Accessed: 2018-03-12]. DOI: https://doi.org/10.3311/PPci.11100.

Pappalardo et al. 2016 – Pappalardo, G., Mineo, S. and Monaco, C. 2016. Geotechnical characterization of limestones employed for the reconstruction of a UNESCO worl heritage Baroque monument in southeastern Sicily (Italy). *Engineering Geology* 212, pp. 86–97.

Penkalowa, B. 1963. Limestone of the Pińczów-Wójczański range and marl in the monuments of Wiślica (*Wapienie pasma pińczowsko-wójczańskiego i margle w zabytkach Wiślicy*) [In:] Budkowa Z. et al. Discoveries in Wiślica (*Odkrycia w Wiślicy*). *Rozprawy Zespołu Badań nad Polskim Średniowieczem Uniwersytetu Warszawskiego i Politechniki Warszawskiej*. Cz. I, Warszawa: PWN, pp. 215–247 (*in Polish*).

Peszat, C. 1984. Variability of the petrographic and mineral composition of Cergowa sandstones in the context of their deposition and diagenetic transformations (*Zmienność składu petrograficzno-mineralnego piaskowców cergowskich na tle warunków ich depozycji i przemian diagenetycznych*). *Biuletyn Instytutu Geologicznego* 346, pp. 208–239 (*in Polish*).

Pinińska, J. ed. 1994. Strength and deformation properties of rocks. Vol. I. Sedimentary rocks of the Świętokrzyskie region (*Właściwości wytrzymałościowe i odkształceniowe skał.* Cz. I. *Skały osadowe regionu świętokrzyskiego*). Zakład Geomechaniki Instytutu Hydrogeologii i Geologii Inżynierskiej, Warszawa (*in Polish*).

van der Plas, L. and Tobi, A.C. 1965. A chart for judging the reliability of point counting results. *Amer. J. Sci.* 263, 87–90.

Plewa, M. and Plewa, S. 1992. Petrophysics (*Petrofizyka*). Warszawa: Wydawnictwa Geologiczne (*in Polish*).

PN-EN 1925. Natural stone test methods. Determination of water absorption coefficient by capillarity.

PN-EN 1926. Natural stone test methods. Determination of uniaxial compressive strength.

PN-EN 1936. Natural stone test methods. Determination of real density and apparent density, and of total and open porosity.

PN-EN 13755. Natural stone test methods. Determination of water absorption at atmospheric pressure.

PN-EN 14579. Natural stone test methods. Determination of sound speed propagation.

Přikryl, R. 2001. Some microstructural aspects of strength variation in rocks. *International Journal of Rock Mechanics and Mining Sciences* 38, pp. 671–682.

Przybyszewski, K. 2007. Simplified geological documentation of the mineral deposit – light limestone "Włochy" in cat. C1 in the city of Italy (*Uproszczona dokumentacja geologiczna złoża kopaliny pospolitej – wapieni lekkich „Włochy" w kat. C1 w miejscowości Włochy*). Kielce: Przedsiębiorstwo Projektowo-Usługowe „Area" s.c. (*in Polish*).

Przybyszewski, K. and Wnęk-Potowniak, A. 2011. Simplified geological documentation of the mineral deposit – light limestone "Włochy I" in cat. C1 in the city of Włochy, gm. Pińczów, province świętokrzyskie (*Uprosz-*

www.czasopisma.pan.pl PAN POLSKA AKADEMIA NAUK www.journals.pan.pl

czona dokumentacja geologiczna złoża kopaliny pospolitej – wapieni lekkich „Włochy I" w kat. C1 w miejscowości Włochy, gm. Pińczów, woj. świętokrzyskie). Kielce: Przedsiębiorstwo Projektowo-Usługowe „Area" s.c. (*in Polish*).

Radwański, A. 1969. Transgression of the lower torton on the southern slopes of the Świętokrzyskie Mountains (bay zone and their foreland) (*Transgresja dolnego tortonu na południowych stokach Gór Świętokrzyskich (strefa zatok i ich przedpola)*). *Acta Geologica Polonica* 19, 1, pp. 1–164 (*in Polish*).

Rajchel, J. 2014. The apotropaical stony sculptures in Kraków architecture (*Kamienne apotropaiczne rzeźby w architekturze Krakowa*). *Przegląd Geologiczny* 62, 3, 156–163 (*in Polish*).

Rajchel, J. and Myszkowska, J. 1998. Lithology of limestones from Bircza Lithothamnium Limestone Bed (Skole Unit, Outer Flysch Carpathians, southern Poland) (*Litologia wapieni z warstwy wapienia litotamniowego z Birczy (wt) – jednostka skolska, zewnętrzne Karpaty fliszowe*). *Przegląd Geologiczny* 46, 12, pp. 1247–1253 (*in Polish*).

Regnet et al. 2015 – Regnet, J.B., Robion, P., David, C., Fortin, J., Brigaud, B. and Yven, B. 2015. Acoustic and reservoir properties of microporous carbonate rocks: Implication of micrite particle size and morphology. *Journal of Geophysical Research: Solid Earth* 120 (2), pp. 790–811.

Rembiś, M. and Smoleńska, A. 2008. Building stone in selected sacral edifices of the Słomniki region (*Kamień w wybranych obiektach sakralnych rejonu Słomnik*). *Biuletyn PIG* 429, pp. 167–172 (*in Polish*).

Riegl, B. and Piller, W.E. 2000. Biostromal Coral Facies – A Miocene Example from the Leitha Limestone (Austria) and its Actualistic Interpretation. *PALAIOS* 15, pp. 399–413.

Rögl, F. 1998. Palaeogeographic Considerations for Mediterranean and Paratethys Seaways (Oligocene to Miocene). *Annales des Naturhistorischen Museums in Wien* 99A, pp. 279–310.

Rutkowski, J. 1976. Detrimental Sarmatian settlements on the southern border of the Świętokrzyskie Mountains (*Detrytyczne osady sarmatu na południowym obrzeżeniu Gór Świętokrzyskich*). *Prace Geologiczne PAN* 100 (*in Polish*).

Rutkowski, J. 1980. On the volumetric density of the Miocene limestone near Pińczów and Staszów (*O zmienności gęstości objętościowej wapieni miocenu okolic Pińczowa i Staszowa*). *Sprawozdania z Posiedzień Komisji Naukowych PAN, Oddział Kraków* 21, 2, pp. 111–113 (*in Polish*).

Rydzewski, A. 1975. Microfaced petrographic studies of Lower-Lithuanian calcareous limestone wójczowsko-pińczowskiego range (*Mikrofacjalne badania petrograficzne dolnotortońskich wapieni litotamniowych pasma wójczowsko-pińczowskiego*). *Przegląd Geologiczny* 23, 1, pp. 8–12 (*in Polish*).

Senkowicz, E. 1958. Detailed Geological Map of Poland on a scale of 1: 50000. Sheet of Pińczów (*Szczegółowa Mapa Geologiczna Polski w skali 1:50000. Arkusz Pińczów*). Warszawa: Wydawnictwa Geologiczne (*in Polish*).

Smoleńska, A. and Rembiś, M. 1999. The State of the Preservation of Pińczów Limestone Applied in Decorative Architectonic Elements of the Church of the Holy Virgin Mary in Cracow (*Stan zachowania wapienia pińczowskiego zastosowanego w dekoracyjnych elementach architektonicznych kościoła Mariackiego w Krakowie*). *Ochrona Zabytków* 52, 2. pp. 122–126 (*in Polish*).

Stańczak, G. 2008. Origin of variability of reservoir properties of the early cretaceous Węglówka sandstone (Outer Carpathians) (*Charakter i geneza zmienności właściwości zbiornikowych dolnokredowych piaskowców węglowieckich (Karpaty zewnętrzne)*). *Biuletyn PIG* 429, pp. 195–202 (*in Polish*).

Stańczak, G. and Figarska-Warchoł, B. 2016. Grain-size analysis of sandstones: an effect of thin-section orientation and selection of mineral components (*Wpływ orientacji szlifu mikroskopowego i wyboru mierzonych składników mineralnych na wyniki analizy granulometrycznej*). *Górnictwo Odkrywkowe* 57, 5, pp. 42–52 (*in Polish*).

Studencki, W. 1979. Paleogeography of the Lower Badenian of the Wójcza-Pińczów range (*Paleogeografia dolnego badenu garbu wójczańsko-pińczowskiego*). *Przegląd Geologiczny* 27, 1, pp. 10–13 (*in Polish*).

Studencki, W. 1988a. Facies and sedimentary environment of the Pinczów Limestones (Middle Miocene; Holy Cross Mountains, Central Poland). *Facies* 18, pp. 1–26.

Studencki, W. 1988b. Red Algae from the Pińczów Limestones (Middle Miocene, Świętokrzyskie Mountains, Poland). *Acta Palaeontologica Polonica* 33, 1, pp. 3–57.

Studencki, W. 1999. Red-algal limestones in the Middle Miocene of the Carpathian Foredeep in Poland: facies variability and palaeoclimatic implications. *Geological Quarterly* 43, 4, pp. 395–404.

www.czasopisma.pan.pl PAN POLSKA AKADEMIA NAUK www.journals.pan.pl

Szuflicki et al. eds. 2017 – Szuflicki, M., Malon, A. and Tymiński, M. eds. 2017. Resource balance Mineral deposits in Poland as at December 31, 2016 (*Bilans Zasobów Złóż Kopalin w Polsce wg stanu na 31 XII 2016 r.*) Warszawa: Państwowy Instytut Geologiczny – Państwowy Instytut Badawczy (*in Polish*).

Török, Á. 2003. Surface strength and mineralogy of weathering crusts on limestone buildings in Budapest. *Building and Environment* 38, pp. 1185–1192.

Török et al. 2004 – Török, Á., Rozgonyi, N., Přikryl, R. and Přikrylová, J. 2004. *Leithakalk: the ornamental and building stone of Central Europe, an overview* [In:] Přikryl, R. ed. *Dimension Stone. New perspectives for a traditional building material*. Rotterdam: Balkema pp. 89–93.

Török, Á. and Vásárhelyi, B. 2010. The influence of fabric and water content on selected rock mechanical parameters of travertine, examples from Hungary. *Engineering Geology* 115, pp. 237–245.

Urban, J. and Gągol, J. 2015. History of prospection and use of mineral resources in the Ponidzie region (*Tradycje poszukiwań i wykorzystania surowców mineralnych na Ponidziu*). *Przegląd Geologiczny* 63, 8, pp. 475–484 (*in Polish*).

Weber-Kozińska, M. 1963. Work on the identification of stones in the monuments of Wiślica (*Prace nad identyfikacją kamieni w zabytkach wiślickich*) [In:] Budkowa Z. et al. Discoveries in Wiślica (*Odkrycia w Wiślicy*). *Rozprawy Zespołu Badań nad Polskim Średniowieczem Uniwersytetu Warszawskiego i Politechniki Warszawskiej* Cz. I., Warszawa: PWN, pp. 251–269 (*in Polish*).

Wiedl et al. 2012 – Wiedl, T., Harzhauser, M. and Piller W.E. 2012. Facies and synsedimentary tectonics on a Badenian carbonate platform in the southern Vienna Basin (Austria, Central Parathetys). *Facies* 58, pp. 523–548.

Wysocka et al. 2016 – Wysocka, A., Radwański, A., Górka, M., Bąbel, M., Radwańska, U. and Złotnik, M. 2016. The Middle Miocene of the Fore-Carpathian Basin (Poland, Ukraine and Moldova). *Acta Geologica Polonica* 66, 3, pp. 351–401.

THE EFFECT OF PETROGRAPHIC CHARACTERISTICS ON PHYSICAL AND MECHANICAL PROPERTIES OF CURRENTLY EXPLOITED PIŃCZÓW LIMESTONES – A TYPE OF LEITHA LIMESTONES (CARPATHIAN FOREDEEP, SOUTHERN POLAND)

Keywords

Middle Miocene, SEM-EDS, capillary water absorption, ultrasonic wave velocity, uniaxial compressive strength, dimension stone

Abstract

The subject of the research was the Middle Miocene red algal limestone from the Włochy deposit, which is currently the only place of exploitation of the Pińczów Limestone representing a local type of the Leitha Limestone. The collected samples of this rock belong to the organodetric facies of diverse grain size and sorting of clastic material. Considering the proportions of characteristic skeleton remains, the composition of the coarse-grained organodetric facies is red algal-foraminiferalbryozoic, while of the fine-grained facies is foraminiferal-red algal. The cement of these rocks is predominantly sparite compared to micrite-clay matrix. A complement to petrographic studies was the chemical analysis and identification of mineral phases with X-ray diffraction. Moreover, physical and mechanical properties of samples were analyzed. Porosity of the rock was assessed in the polarizing and scanning microscope (SEM-EDS) observations, as well as with a porosimetric tests. The coarse-detrital limestone with a dominant binder in the form of intergranular cement is characterized by the apparent density sometimes exceeded 1.90 Mg/m^3, while fine-grained limestone has the highest water absor-

www.czasopisma.pan.pl PAN POLSKA AKADEMIA NAUK www.journals.pan.pl

bability (above 20%) and total porosity (about 40%). The above properties influenced high water absorption by capillarity, limiting the possibility of using limestone in places exposed to moisture. The observed relationship between the ultrasonic waves velocity and the uniaxial compressive strength gives the possibility of predicting the value of the latter parameter in the future. The limestones from Włochy deposit do not differ in quality from the previously used Pińczów Limestones, and their technical parameters predestine them for use as cladding material with insulating properties.

CHARAKTERYSTYKA PETROGRAFICZNA A WŁAŚCIWOŚCI FIZYCZNO-MECHANICZNE AKTUALNIE EKSPLOATOWANYCH WAPIENI PIŃCZOWSKICH – ODMIANY WAPIENI LITAWSKICH (ZAPADLISKO PRZEDKARPACKIE, POŁUDNIOWA POLSKA)

Słowa kluczowe

środkowy miocen, SEM-EDS, kapilarna absorpcja wody, prędkość fali ultradźwiękowej, jednoosiowa wytrzymałość na ściskanie, kamień wymiarowy

Streszczenie

Przedmiotem badań były środkowomioceńskie wapienie krasnorostowe ze złoża Włochy, jedynego obecnie miejsca eksploatacji wapieni pińczowskich, reprezentujących lokalny typ wapieni litawskich. Pobrane próbki tych skał reprezentują fację organodetrytyczną o zróżnicowanym uziarnieniu i wysortowaniu materiału okruchowego. Biorąc pod uwagę proporcje charakterystycznych szczątków szkieletowych, skład facji gruboziarnistej jest krasnorostowo-otwornicowo-mszywiołowy, zaś drobnoziarnistej – otwornicowo-krasnorostowy. Spoiwo tych skał stanowi cement sparytowy, przeważający nad matriks mikrytowo-ilastą. Uzupełnieniem obserwacji petrograficznych była analiza składu chemicznego i identyfikacja faz mineralnych przy pomocy dyfraktometrii rentgenowskiej (XRD). Ponadto wykonano badania właściwości fizycznych i mechanicznych. Porowatość skały oceniono na podstawie obserwacji w mikroskopie polaryzacyjnym i skaningowym (SEM-EDS) oraz w testach porozymetrycznych. Wapienie grubodetrytyczne z dominującym spoiwem w postaci cementu intergranularnego odznaczają się gęstością pozorną przekraczającą czasem 1,90 Mg/m^3, podczas gdy drobnoziarniste mają najwyższą nasiąkliwość wagową (pow. 20%) i porowatość całkowitą (ok. 40%). Wpływa to na wysoką nasiąkliwość kapilarną, ograniczającą możliwości zastosowania wapienia w miejscach narażonych na zawilgocenia. Stwierdzona zależność pomiędzy prędkością fal ultradźwiękowych a wytrzymałością na ściskanie jednoosiowe daje możliwość prognozowania wartości tego ostatniego parametru w przyszłości. Wapienie ze złoża Włochy mają jakość podobną do innych wapieni pińczowskich eksploatowanych w przeszłości, a ich parametry techniczne predestynują je do zastosowania jako materiału okładzinowego o właściwościach izolacyjnych.